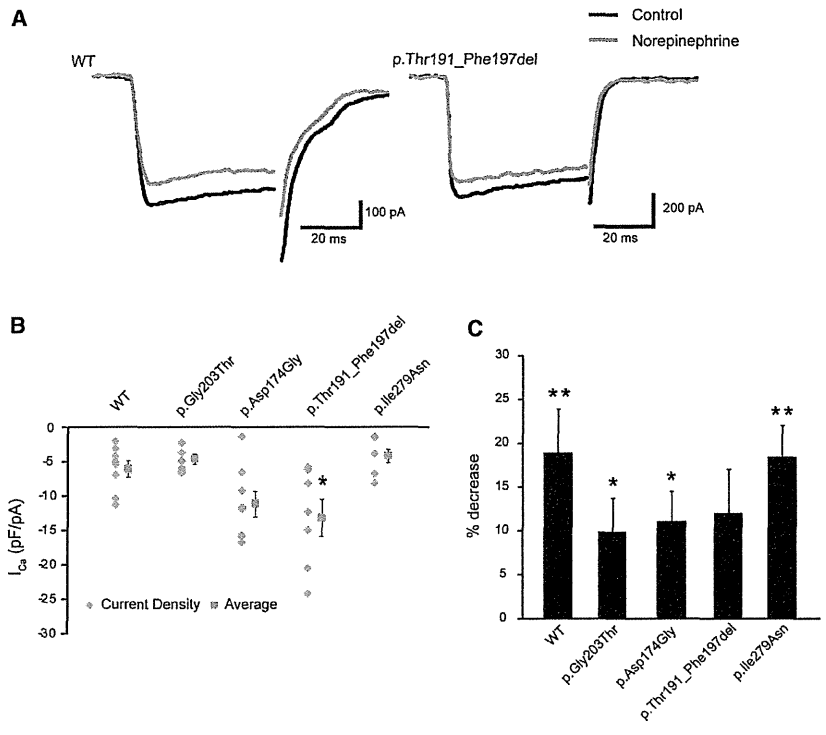

Figure 5. Evaluation of $G\alpha_o$-Mediated Signaling in NG108-15 Cell Calcium-Current Generation

(A) Representative traces of voltage-gated calcium currents generated in NG108-15 cells expressing WT (left) or p.Thr191_Phe197del altered (right) $G\alpha_{o1}$. Black and red traces represent the currents before and 3 min after application of 10 μM norepinephrine, respectively.

(B) Current densities of the calcium currents before norepinephrine treatment in cells expressing WT or altered $G\alpha_{o1}$. Scatter plots represent the densities in individual cells. Red squares and bars represent the means and SEMs, respectively, of the densities in individual cell groups (WT, n = 8; p.Gly203Thr, n = 7; p.Asp174Gly, n = 8; p.Thr191_Phe197del, n = 7; p.Ile279Asn, n = 7). Compared with that in cells expressing WT $G\alpha_{o1}$, the current density in cells expressing p.Thr191_Phe197del increased significantly (*$p < 0.05$ by Dunnett's post hoc test). The densities in the cells expressing other altered proteins did not vary significantly.

(C) Comparison of norepinephrine-induced inhibition of calcium currents in cells expressing altered $G\alpha_{o1}$. Each error bar represents the mean and SEM of the percent decrease in current density induced by application of 10 μM norepinephrine. Paired t tests indicated that the inhibition induced by norepinephrine was significant in cells expressing WT (n = 8) and p.Gly203Thr (n = 7), p.Asp174Gly (n = 8), and p.Ile279Asn (n = 7) altered proteins (**$p < 0.01$ and *$p < 0.05$), but not in cells expressing p.Thr191_Phe197del (n = 7). Although there was some tendency for decreased inhibition in cells expressing altered proteins, the tendency did not reach statistical significance compared with that in WT-expressing cells ($p = 0.41$ by ANOVA).

and p.Asp174Gly) also showed weak signal in the cytosol, suggesting that localization to the plasma membrane was variably impaired in three altered proteins. Measurement of voltage-dependent calcium currents in NG108-15 cells also suggested impaired functions of altered $G\alpha_{o1}$. The p.Thr191_Phe197del alteration significantly increased the basal calcium-current density, and compared with WT-expressing cells, cells expressing one of the three substitutions (p.Thr191_Phe197del, p.Asp174Gly, or p.Gly203Thr) showed a tendency towards weaker inhibition of calcium currents by norepinephrine. All these data suggest that the four *GNAO1* mutations might cause loss of $G\alpha_{o1}$ function.

Our experimental data suggest that $G\alpha_o$ function might be most severely affected in the p.Thr191_Phe197del altered protein. This appears to be correlated with the severity of clinical features because individual 3 showed both OS and involuntary movements and indeed died during the infantile period. Therefore, she might have had the most severe phenotype caused by a *GNAO1* mutation. Another interesting finding is somatic mosaicism of the c.521A>G (p.Asp174Gly) mutation in individual 2, in whom approximately 35%–50% of cells harbored the mutation. Somatic mosaicism of responsive genes in infantile epilepsy, such as *SCN1A* (MIM 182389) and *STXBP1*, have been reported, explaining the presence of unaffected or mildly affected transmitting parents.[30,31] However, individual 2 showed OS, delayed myelination, and thin corpus callosum. Although we did not determine the mosaic rate in brain tissues, the presence of 35%–50% of cells harboring the *GNAO1* mutation in the brain might be sufficient to cause abnormal brain development.

It has been reported that activation of G-protein-coupled α_2 adrenergic receptors by norepinephrine attenuates epileptiform activity in the hippocampal CA3 region.[32] $G\alpha_o$ is known to be involved in this response,[33] suggesting that alteration of pathways mediated by α_2 adrenergic receptor and $G\alpha_o$ might contribute to the pathogenesis of epilepsy. Because calcium-current inhibition is a well-known consequence of $G\alpha_o$-mediated signaling induced by norepinephrine, it is possible that epileptic seizures associated with *GNAO1* mutations might be improved by calcium-channel modulators. For example, pregabalin and gabapentin act as selective calcium-channel blockers,[34,35] and topiramate modulates high-voltage-activated calcium channels in dentate granule cells.[36] Because our four individuals were not treated with these drugs, it is worth administrating these three drugs for examining putative protective effects.

In conclusion, de novo heterozygous *GNAO1* mutations were identified in four individuals with epileptic encephalopathy. Furthering our understanding of abnormal

$G\alpha_o$-mediated heterotrimeric G protein signaling might provide new insights into the pathogenesis and treatment of epileptic encephalopathy.

Supplemental Data

Supplemental Data include two figures, three tables, and one movie and can be found with this article online at http://www.cell.com/AJHG.

Acknowledgments

We would like to thank the individuals and their families for their participation in this study. We also thank Aya Narita and Nobuko Watanabe for their technical assistance and Tohru Kozasa and Nobuchika Suzuki for their valuable comments. This work was supported by the Ministry of Health, Labour, and Welfare of Japan, the Japan Society for the Promotion of Science (Grants-in-Aid for Scientific Research (B) [25293085 and 25293235] and a Grant-in-Aid for Scientific Research (A) [13313587]), the Takeda Science Foundation, the Japan Science and Technology Agency, the Strategic Research Program for Brain Sciences (11105137), and a Grant-in-Aid for Scientific Research on Innovative Areas (Transcription Cycle) from the Ministry of Education, Culture, Sports, Science, and Technology of Japan (12024421).

Received: May 17, 2013
Revised: July 9, 2013
Accepted: July 17, 2013
Published: August 29, 2013

Web Resources

The URLs for data presented herein are as follows:

CLUSTALW, http://www.genome.jp/tools/clustalw/
GenBank, http://www.ncbi.nlm.nih.gov/Genbank/
NHLBI Exome Sequencing Project (ESP) Exome Variant Server, http://evs.gs.washington.edu/EVS/
Online Mendelian Inheritance in Man (OMIM), http://www.omim.org/
Picard, http://picard.sourceforge.net/
Protein Data Bank, http://www.rcsb.org/pdb/home/home.do
PyMOL, www.pymol.org
RefSeq, http://www.ncbi.nlm.nih.gov/RefSeq
UniProtKB/Swiss-Prot, http://www.uniprot.org/

References

1. Dulac, O. (2001). Epileptic encephalopathy. Epilepsia *42* (*Suppl 3*), 23–26.
2. Ohtahara, S., and Yamatogi, Y. (2006). Ohtahara syndrome: with special reference to its developmental aspects for differentiating from early myoclonic encephalopathy. Epilepsy Res. *70* (*Suppl 1*), S58–S67.
3. Saitsu, H., Kato, M., Koide, A., Goto, T., Fujita, T., Nishiyama, K., Tsurusaki, Y., Doi, H., Miyake, N., Hayasaka, K., and Matsumoto, N. (2012). Whole exome sequencing identifies *KCNQ2* mutations in Ohtahara syndrome. Ann. Neurol. *72*, 298–300.
4. Saitsu, H., Kato, M., Mizuguchi, T., Hamada, K., Osaka, H., Tohyama, J., Uruno, K., Kumada, S., Nishiyama, K., Nishimura, A., et al. (2008). *De novo* mutations in the gene encoding STXBP1 (MUNC18-1) cause early infantile epileptic encephalopathy. Nat. Genet. *40*, 782–788.
5. Weckhuysen, S., Mandelstam, S., Suls, A., Audenaert, D., Deconinck, T., Claes, L.R., Deprez, L., Smets, K., Hristova, D., Yordanova, I., et al. (2012). *KCNQ2* encephalopathy: emerging phenotype of a neonatal epileptic encephalopathy. Ann. Neurol. *71*, 15–25.
6. Kato, M., Saitoh, S., Kamei, A., Shiraishi, H., Ueda, Y., Akasaka, M., Tohyama, J., Akasaka, N., and Hayasaka, K. (2007). A longer polyalanine expansion mutation in the *ARX* gene causes early infantile epileptic encephalopathy with suppression-burst pattern (Ohtahara syndrome). Am. J. Hum. Genet. *81*, 361–366.
7. Wettschureck, N., and Offermanns, S. (2005). Mammalian G proteins and their cell type specific functions. Physiol. Rev. *85*, 1159–1204.
8. Huff, R.M., Axton, J.M., and Neer, E.J. (1985). Physical and immunological characterization of a guanine nucleotide-binding protein purified from bovine cerebral cortex. J. Biol. Chem. *260*, 10864–10871.
9. Valenzuela, D., Han, X., Mende, U., Fankhauser, C., Mashimo, H., Huang, P., Pfeffer, J., Neer, E.J., and Fishman, M.C. (1997). G alpha(o) is necessary for muscarinic regulation of Ca2+ channels in mouse heart. Proc. Natl. Acad. Sci. USA *94*, 1727–1732.
10. Jiang, M., Gold, M.S., Boulay, G., Spicher, K., Peyton, M., Brabet, P., Srinivasan, Y., Rudolph, U., Ellison, G., and Birnbaumer, L. (1998). Multiple neurological abnormalities in mice deficient in the G protein Go. Proc. Natl. Acad. Sci. USA *95*, 3269–3274.
11. Saitsu, H., Kato, M., Osaka, H., Moriyama, N., Horita, H., Nishiyama, K., Yoneda, Y., Kondo, Y., Tsurusaki, Y., Doi, H., et al. (2012). *CASK* aberrations in male patients with Ohtahara syndrome and cerebellar hypoplasia. Epilepsia *53*, 1441–1449.
12. Saitsu, H., Nishimura, T., Muramatsu, K., Kodera, H., Kumada, S., Sugai, K., Kasai-Yoshida, E., Sawaura, N., Nishida, H., Hoshino, A., et al. (2013). *De novo* mutations in the autophagy gene *WDR45* cause static encephalopathy of childhood with neurodegeneration in adulthood. Nat. Genet. *45*, 445–449, e1.
13. DePristo, M.A., Banks, E., Poplin, R., Garimella, K.V., Maguire, J.R., Hartl, C., Philippakis, A.A., del Angel, G., Rivas, M.A., Hanna, M., et al. (2011). A framework for variation discovery and genotyping using next-generation DNA sequencing data. Nat. Genet. *43*, 491–498.
14. Wang, K., Li, M., and Hakonarson, H. (2010). ANNOVAR: functional annotation of genetic variants from high-throughput sequencing data. Nucleic Acids Res. *38*, e164.
15. Robinson, J.T., Thorvaldsdóttir, H., Winckler, W., Guttman, M., Lander, E.S., Getz, G., and Mesirov, J.P. (2011). Integrative genomics viewer. Nat. Biotechnol. *29*, 24–26.
16. Thorvaldsdóttir, H., Robinson, J.T., and Mesirov, J.P. (2013). Integrative Genomics Viewer (IGV): high-performance genomics data visualization and exploration. Brief. Bioinform. *14*, 178–192.
17. Slepak, V.Z., Wilkie, T.M., and Simon, M.I. (1993). Mutational analysis of G protein alpha subunit G(o) alpha expressed in Escherichia coli. J. Biol. Chem. *268*, 1414–1423.
18. Williams, D.J., Puhl, H.L., and Ikeda, S.R. (2010). A Simple, Highly Efficient Method for Heterologous Expression in Mammalian Primary Neurons Using Cationic Lipid-mediated mRNA Transfection. Front Neurosci. *4*, 181.

19. Guerois, R., Nielsen, J.E., and Serrano, L. (2002). Predicting changes in the stability of proteins and protein complexes: a study of more than 1000 mutations. J. Mol. Biol. *320*, 369–387.
20. Wall, M.A., Coleman, D.E., Lee, E., Iñiguez-Lluhi, J.A., Posner, B.A., Gilman, A.G., and Sprang, S.R. (1995). The structure of the G protein heterotrimer Gi alpha 1 beta 1 gamma 2. Cell *83*, 1047–1058.
21. Rasmussen, S.G., DeVree, B.T., Zou, Y., Kruse, A.C., Chung, K.Y., Kobilka, T.S., Thian, F.S., Chae, P.S., Pardon, E., Calinski, D., et al. (2011). Crystal structure of the β2 adrenergic receptor-Gs protein complex. Nature *477*, 549–555.
22. Waldo, G.L., Ricks, T.K., Hicks, S.N., Cheever, M.L., Kawano, T., Tsuboi, K., Wang, X., Montell, C., Kozasa, T., Sondek, J., and Harden, T.K. (2010). Kinetic scaffolding mediated by a phospholipase C-beta and Gq signaling complex. Science *330*, 974–980.
23. Edvardson, S., Baumann, A.M., Mühlenhoff, M., Stephan, O., Kuss, A.W., Shaag, A., He, L., Zenvirt, S., Tanzi, R., Gerardy-Schahn, R., and Elpeleg, O. (2013). West syndrome caused by ST3Gal-III deficiency. Epilepsia *54*, e24–e27.
24. Molinari, F., Raas-Rothschild, A., Rio, M., Fiermonte, G., Encha-Razavi, F., Palmieri, L., Palmieri, F., Ben-Neriah, Z., Kadhom, N., Vekemans, M., et al. (2005). Impaired mitochondrial glutamate transport in autosomal recessive neonatal myoclonic epilepsy. Am. J. Hum. Genet. *76*, 334–339.
25. Mills, P.B., Surtees, R.A., Champion, M.P., Beesley, C.E., Dalton, N., Scambler, P.J., Heales, S.J., Briddon, A., Scheimberg, I., Hoffmann, G.F., et al. (2005). Neonatal epileptic encephalopathy caused by mutations in the PNPO gene encoding pyridox(am)ine 5′-phosphate oxidase. Hum. Mol. Genet. *14*, 1077–1086.
26. Shen, J., Gilmore, E.C., Marshall, C.A., Haddadin, M., Reynolds, J.J., Eyaid, W., Bodell, A., Barry, B., Gleason, D., Allen, K., et al. (2010). Mutations in PNKP cause microcephaly, seizures and defects in DNA repair. Nat. Genet. *42*, 245–249.
27. Kurian, M.A., Meyer, E., Vassallo, G., Morgan, N.V., Prakash, N., Pasha, S., Hai, N.A., Shuib, S., Rahman, F., Wassmer, E., et al. (2010). Phospholipase C beta 1 deficiency is associated with early-onset epileptic encephalopathy. Brain *133*, 2964–2970.
28. Nakata, H., and Kozasa, T. (2005). Functional characterization of Galphao signaling through G protein-regulated inducer of neurite outgrowth 1. Mol. Pharmacol. *67*, 695–702.
29. McFadzean, I., Mullaney, I., Brown, D.A., and Milligan, G. (1989). Antibodies to the GTP binding protein, Go, antagonize noradrenaline-induced calcium current inhibition in NG108-15 hybrid cells. Neuron *3*, 177–182.
30. Saitsu, H., Hoshino, H., Kato, M., Nishiyama, K., Okada, I., Yoneda, Y., Tsurusaki, Y., Doi, H., Miyake, N., Kubota, M., et al. (2011). Paternal mosaicism of an *STXBP1* mutation in OS. Clin. Genet. *80*, 484–488.
31. Marini, C., Scheffer, I.E., Nabbout, R., Suls, A., De Jonghe, P., Zara, F., and Guerrini, R. (2011). The genetics of Dravet syndrome. Epilepsia *52* (*Suppl 2*), 24–29.
32. Jurgens, C.W., Hammad, H.M., Lichter, J.A., Boese, S.J., Nelson, B.W., Goldenstein, B.L., Davis, K.L., Xu, K., Hillman, K.L., Porter, J.E., and Doze, V.A. (2007). Alpha2A adrenergic receptor activation inhibits epileptiform activity in the rat hippocampal CA3 region. Mol. Pharmacol. *71*, 1572–1581.
33. Goldenstein, B.L., Nelson, B.W., Xu, K., Luger, E.J., Pribula, J.A., Wald, J.M., O'Shea, L.A., Weinshenker, D., Charbeneau, R.A., Huang, X., et al. (2009). Regulator of G protein signaling protein suppression of Galphao protein-mediated alpha2A adrenergic receptor inhibition of mouse hippocampal CA3 epileptiform activity. Mol. Pharmacol. *75*, 1222–1230.
34. Sills, G.J. (2006). The mechanisms of action of gabapentin and pregabalin. Curr. Opin. Pharmacol. *6*, 108–113.
35. Stefani, A., Spadoni, F., Giacomini, P., Lavaroni, F., and Bernardi, G. (2001). The effects of gabapentin on different ligand- and voltage-gated currents in isolated cortical neurons. Epilepsy Res. *43*, 239–248.
36. Zhang, X., Velumian, A.A., Jones, O.T., and Carlen, P.L. (2000). Modulation of high-voltage-activated calcium channels in dentate granule cells by topiramate. Epilepsia *41* (*Suppl 1*), S52–S60.

Clinical spectrum of *SCN2A* mutations expanding to Ohtahara syndrome

Kazuyuki Nakamura, MD
Mitsuhiro Kato, MD, PhD
Hitoshi Osaka, MD, PhD
Sumimasa Yamashita, MD, PhD
Eiji Nakagawa, MD, PhD
Kazuhiro Haginoya, MD, PhD
Jun Tohyama, MD, PhD
Mitsuko Okuda, MD, PhD
Takahito Wada, MD, PhD
Shuichi Shimakawa, MD, PhD
Katsumi Imai, MD
Saoko Takeshita, MD
Hisako Ishiwata, MD
Dorit Lev, MD
Tally Lerman-Sagie, MD
David E. Cervantes-Barragán, MD
Camilo E. Villarroel, MD
Masaharu Ohfu, MD, PhD
Karin Writzl, MD, PhD
Barbara Gnidovec Stražišar, MD, PhD
Shinichi Hirabayashi, MD, PhD
David Chitayat, MD
Diane Myles Reid, MSc
Kiyomi Nishiyama, PhD
Hirofumi Kodera, PhD
Mitsuko Nakashima, MD, PhD
Yoshinori Tsurusaki, PhD
Noriko Miyake, MD, PhD
Kiyoshi Hayasaka, MD, PhD
Naomichi Matsumoto, MD, PhD
Hirotomo Saitsu, MD, PhD

Correspondence to Dr. Matsumoto: naomat@yokohama-cu.ac.jp or Dr. Saitsu: hsaitsu@yokohama-cu.ac.jp

Supplemental data at www.neurology.org

ABSTRACT

Objective: We aimed to investigate the possible association between *SCN2A* mutations and early-onset epileptic encephalopathies (EOEEs).

Methods: We recruited a total of 328 patients with EOEE, including 67 patients with Ohtahara syndrome (OS) and 150 with West syndrome. *SCN2A* mutations were examined using high resolution melt analysis or whole exome sequencing.

Results: We found 14 novel *SCN2A* missense mutations in 15 patients: 9 of 67 OS cases (13.4%), 1 of 150 West syndrome cases (0.67%), and 5 of 111 with unclassified EOEEs (4.5%). Twelve of the 14 mutations were confirmed as de novo, and all mutations were absent in 212 control exomes. A de novo mosaic mutation (c.3976G>C) with a mutant allele frequency of 18% was detected in one patient. One mutation (c.634A>G) was found in transcript variant 3, which is a neonatal isoform. All 9 mutations in patients with OS were located in linker regions between 2 transmembrane segments. In 7 of the 9 patients with OS, EEG findings transitioned from suppression-burst pattern to hypsarrhythmia. All 15 of the patients with novel *SCN2A* missense mutations had intractable seizures; 3 of them were seizure-free at the last medical examination. All patients showed severe developmental delay.

Conclusions: Our study confirmed that *SCN2A* mutations are an important genetic cause of OS. Given the wide clinical spectrum associated with *SCN2A* mutations, genetic testing for *SCN2A* should be considered for children with different epileptic conditions. ***Neurology*® 2013;81:992-998**

GLOSSARY

BFNIS = benign familial neonatal-infantile seizures; **DS** = Dravet syndrome; **EOEE** = early-onset epileptic encephalopathy; **HRM** = high resolution melt; **OS** = Ohtahara syndrome; **WES** = whole exome sequencing; **WS** = West syndrome.

Early-onset epileptic encephalopathies (EOEEs) include Ohtahara syndrome (OS), early myoclonic epileptic encephalopathy, West syndrome (WS), Dravet syndrome (DS), and other diseases.[1,2] OS is characterized by an early onset of spasms, mainly in the neonatal period, intractable seizures, and a suppression-burst pattern on EEG.[3] WS is characterized by spasms, an EEG finding termed hypsarrhythmia, and arrest of psychomotor development.[4] De novo mutations in *STXBP1*, *KCNQ2*, *CDKL5*, *ARX*, and *SPTAN1* are known causes of OS and WS.[5–11]

Voltage-gated sodium channels consist of 1 α subunit and 1 or 2 β subunits. The α subunit forms a pore structure, and is composed of 4 domains (domains I–IV), each containing 5 hydrophobic segments (S1, S2, S3, S5, S6) and 1 positively charged segment (S4).[12] The voltage-gated sodium channel repertoire in humans includes 9 α subunits ($Na_v1.1$–$Na_v1.9$). $Na_v1.1$, $Na_v1.2$, $Na_v1.3$, and $Na_v1.6$, encoded by *SCN1A*, *SCN2A*, *SCN3A*, and *SCN8A*,

From the Department of Human Genetics (K. Nakamura, K. Nishiyama, H.K., M.N., Y.T., N. Miyake, N. Matsumoto, H.S.), Yokohama City University Graduate School of Medicine, Yokohama; Department of Pediatrics (K. Nakamura, M.K., K. Hayasaka), Yamagata University Faculty of Medicine, Yamagata; Division of Neurology (H.O., S.Y., M. Okuda, T.W.), Clinical Research Institute, Kanagawa Children's Medical Center, Yokohama; Department of Child Neurology (E.N.), National Center Hospital, National Center of Neurology and Psychiatry, Tokyo; Department of Pediatric Neurology (K. Haginoya), Takuto Rehabilitation Center for Children, Sendai; Department of Pediatrics (J.T.), Epilepsy Center, Nishi-Niigata Chuo National Hospital, Niigata; Department of Pediatrics (S.S.), Osaka Medical College Hospital, Osaka; National Epilepsy Center (K.I.), Shizuoka Institute of Epilepsy and Neurological Disorders, Shizuoka; Department of Pediatrics (S.T.), Yokohama City University Medical Center, Yokohama; Department of Pediatrics (H.I.), Tokyo Metropolitan Bokuto Hospital, Tokyo, Japan; Metabolic Neurogenetic Clinic (D.L., T.L.-S.), Wolfson Medical Center, Holon, Israel; Department of Human Genetics (D.E.C.-B., C.E.V.), National Institute of Pediatrics, Mexico City, Mexico; Division of Child Neurology (M. Ohfu), Okinawa Nanbu Medical Center and Children's Medical Center, Okinawa, Japan; Institute of Medical Genetics (K.W.), University Medical Center Ljubljana; Department of Child, Adolescent and Developmental Neurology (B.G.S.), University Children's Hospital, Ljubljana, Slovenia; Department of Neurology (S.H.), Nagano Children's Hospital, Nagano, Japan; Department of Obstetrics and Gynecology (D.C.), The Prenatal Diagnosis and Medical Genetics Program, Mount Sinai Hospital, University of Toronto; and Division of Clinical and Metabolic Genetics (D.C., D.M.R.), The Hospital for Sick Children, University of Toronto, Canada.

Go to Neurology.org for full disclosures. Funding information and disclosures deemed relevant by the authors, if any, are provided at the end of the article.

respectively, are highly expressed in the human brain,[13] and mutations can cause epilepsies and psychiatric disorders.[14–17]

Most *SCN2A* mutations cause benign phenotypes such as benign familial neonatal-infantile seizures (BFNIS),[18] and are usually inherited from an affected parent. In contrast, several de novo *SCN2A* mutations have been reported to cause more severe phenotypes,[14,19–22] suggesting a possible involvement in severe epileptic encephalopathies.

To elucidate the genetic basis of OS, we performed exome sequencing and found a de novo *SCN2A* mutation. Subsequently, we screened patients with EOEE for *SCN2A* mutations, and found that de novo *SCN2A* mutations contributed to the development of severe epileptic encephalopathies.

METHODS

Patients. A total of 328 patients with EOEE (67 patients with OS, 150 with WS, and 111 with unclassified EOEE) were analyzed for *SCN2A* mutations. The 67 patients with OS consisted of 44 Japanese and 23 non-Japanese (from other countries). The diagnosis was made based on clinical features and characteristic patterns on EEG. In 257 patients, mutations in *STXBP1* and *KCNQ2* had been excluded by high resolution melt (HRM) analysis in advance. Mutation analysis was performed by HRM analysis or direct sequencing, and 41 of the 328 patients (32 with OS, 4 with WS, and 5 with unclassified EOEEs) were also analyzed by whole exome sequencing (WES). We obtained detailed clinical data from all patients with *SCN2A* mutations, including brain MRI/CT and EEG findings.

Mutation screening. Genomic DNA was obtained from peripheral blood leukocytes by standard methods. DNA for mutation screening was amplified using the Illustra GenomiPhi V2 DNA Amplification Kit (GE Healthcare Japan, Tokyo, Japan). Mutation screening of exons 2 to 27 (including exon 6A) covering the *SCN2A* coding regions (transcript variant 1, NM_021007.2) and exon 6N of transcript variant 3 (NM_001040143.1) was performed by HRM analysis or by direct sequencing of part of exon 27. The DNA of patient 10 from nails and hairs was isolated using ISOHAIR (Nippon Gene, Tokyo, Japan), and DNA in saliva was isolated using Oragene (DNA Genotek, Kanata, Canada). Real-time PCR and subsequent HRM analysis were performed using a Light Cycler 480 (Roche Diagnostics, Otsu, Japan). Samples showing an aberrant melting curve in the HRM analysis were sequenced. PCR primers and conditions are shown in table e-1 on the *Neurology*® Web site at www.neurology.org. All novel mutations were verified using original genomic DNA, and searched for in the variant database of our 212 in-house control exomes.

Whole exome sequencing. DNAs were captured using the SureSelect^{XT} Human All Exon v4 Kit (Agilent Technologies, Santa Clara, CA) and sequenced with 4 samples per lane on an Illumina HiSeq 2000 (Illumina, San Diego, CA) with 101–base pair paired-end reads. Image analysis and base calling were performed by sequence control software with real-time analysis and CASAVA software v1.8 (Illumina). Reads were aligned to GRCh37 with Novoalign (Novocraft Technologies, Selangor, Malaysia), and duplicate reads were marked using Picard (http://picard.sourceforge.net/index.shtml) and excluded from downstream analysis. Local realignments around indels and base quality score recalibrations were performed using the Genome Analysis Toolkit (GATK).[23] Single-nucleotide variants and small indels were identified using the GATK, and were annotated using ANNOVAR.[24] All mutations detected by WES were confirmed by Sanger sequencing.

Parentage testing. For the family showing de novo mutations, parentage was confirmed by microsatellite analysis using ABI Prism Linkage Mapping Set version 2.5, MD10 (Life Technologies, Carlsbad, CA). We chose 12 probes for screening (D6S422, D7S493, D8S285, D9S161, D10S208, D11S987, D12S345, D16S503, D17S921, D18S53, D19S220, and D20S196). Appropriate biological parentage was confirmed if 3 or more informative markers were compatible and other markers showed no discrepancy.

Standard protocol approvals, registrations, and patient consents. The experimental protocols were approved by the Institutional Review Boards for Ethical Issues of Yokohama City University School of Medicine and Yamagata University Faculty of Medicine. Informed consent was obtained from the families of all patients.

RESULTS

Identification of *SCN2A* mutations. We previously performed WES of 12 patients with OS, including patient 142 of the current study.[7,25] To systematically find de novo mutations, we additionally analyzed the parents of patient 142 by WES. We found 2 de novo nonsynonymous mutations in patient 142: c.4868C>A (p.T1623N) in *SCN2A* and c.538A>T (p.I180F) in *FHOD1*. Because de novo *SCN2A* mutations have been reported to cause intractable epilepsy,[19,21] the *SCN2A* mutation was highly likely to have caused the OS. In fact, we found a total of 14 mutations in 15 patients: 9 of 67 OS cases (13.4%), 1 of 150 WS cases (0.67%), and 5 of 111 with unclassified EOEEs (4.5%) (table 1). One mutation (c.638T>A) occurred recurrently in 2 patients, and the mutation was confirmed as a de novo event in 1 of the 2 patients. All other mutations except for 2 (c.2995G>A and c.4886G>T; parents were unavailable) occurred de novo. Interestingly, a de novo mosaic mutation (c.3976G>C) was detected by WES in patient 10. The mutant allele frequency was 18% (37/205 alleles) based on read counts of WES. We confirmed mosaicism in hair, nail, and saliva DNA samples (figure e-1). One mutation (c.634A>G [p.N212D]) was found in the transcript variant 3, which is a neonatal isoform. All of the 15 mutations are missense changes that have not been previously reported. They cannot be found in the 6,500 exomes sequenced by the National Heart, Lung, and Blood Institute exome project or among our 212 in-house control exomes. Sorting Intolerant From Tolerant (SIFT), Polyphen2, and Mutation Taster predicted that all mutations would be highly damaging to the structure of $Na_v1.2$ (table e-2). All 9 mutations in patients with OS were located in linker regions between transmembrane segments (figure 1). Six of these mutations were located in a linker between S4 and S5, 2 were located between S3 and S4, and one near the end of S6. One

Table 1 **Clinical features of *SCN2A* mutations**

Patient	Sex	Dx	Mutation, inheritance	Age at onset	Initial epileptic attacks	Initial EEG at onset	Transition of seizure and EEG (age)	Response to treatment	HC-SD (age)	DD	MRI findings (age)
10	F	OS (→WS)	c.3976G>C, p.V1326L (mosaic), de novo	8 d	Spasms	SB	TS, myoclonus (2 y); hypsarrhythmia (4 mo); multifocal spikes (3 y, 2 mo)	Intractable	−0.4 (0 d)	Severe	Cerebral atrophy, delayed myelination (2 y, 2 mo)
18	F	EOEE	c.638T>A, p.V213D, N/A	3 mo	Focal seizure	Focal spikes	TS (7 y)	Intractable	N/A	Severe	Mild cerebellar and cerebral atrophy (6 mo); delayed myelination (9 mo)
99	F	WS	c.2558G>A, p.R853Q, de novo	10 mo	Spasms	Hypsarrhythmia	Multifocal spikes, MISF (1 y, 6 mo); no epileptic discharges (6 y, 2 mo)	Seizure-free after LTG at 6 y, 2 mo	N/A	Severe	Cerebral atrophy (frontal, temporal), cerebellar atrophy, thin CC (4 y, 4 mo)
142	M	OS (→WS)	c.4868C>A, p.T1623N, de novo	1 d	TS	SB	Multifocal spikes (2 mo); spasms (3 mo); hypsarrhythmia (3 mo); mainly slow wave (1 y, 4 mo)	Intractable	−1.1 (1 y, 4 mo)	Severe	Thin CC (3 mo); cerebral atrophy (1 y, 4 mo)
146	F	OS	c.707C>G, p.T236S, de novo	0 d	Focal seizure	SB	MISF (5 mo)	Seizure-free after ZNS, LEV, PHT, VGB	N/A	Severe	Thin CC, white matter atrophy, T2 hyperintensity within globi pallidi (1 y, 3 mo)
185	M	OS (→WS)	c.4007C>A, p.S1336Y, de novo	1 d	Myoclonic, TS	SB	Modified hypsarrhythmia (1 y, 3 mo)	Intractable	−0.4 (1 d)	Severe, died at 5 y	Normal (1 mo)
207	M	OS (→WS)	c.3967A>G, p.M1323V, de novo	13 d	GTCS	SB	Hypsarrhythmia (2.5 mo); multifocal polyspikes (3 mo); TS (5 mo); multifocal spikes (8 y)	Intractable	N/A	Severe	Mild cortical atrophy (7 y)
230	F	OS	c.4013T>C, p.M1338T, de novo	7 d	Spasms	SB	Focal seizure (3 mo); multifocal spikes (11 mo)	Intractable	−2.0 (5 y, 3 mo)	Severe	Normal (1 mo); cerebral atrophy (4 y, 9 mo)
251	F	EOEE	c.638T>A, p.V213D, de novo	1.5 mo	TS	Multifocal spikes	Multifocal spikes and diffuse S-W (14 y)	Intractable	−0.8 (4 mo)	Severe	Delayed myelination, cerebral and cerebellar atrophy (1 y); thin CC (14 y)
252	M	OS (→WS)	c.634A>G (variant 3), p.N212D, de novo	14 d	Pedaling	SB	TS, eyelid myoclonia (3 mo); spasms (4 mo); hypsarrhythmia (3 mo); TS (9 mo)	Intractable	N/A	Severe	Cerebral atrophy (16 d); severe cerebral atrophy, delayed myelination (4 y)
254	F	EOEE	c.506A>G, p.E169G, de novo	6 mo	TS	Multifocal spikes	Febrile seizure (6 mo); myoclonic seizure, focal seizure, TS (1 y)	Intractable	−1.7 (5 y, 8 mo)	Severe	Cerebral atrophy, thin CC (5 y)
255	F	EOEE	c.4886G>T, p.R1629L, N/A	3 d	Focal seizure, myoclonus	Focal spikes	Burst of spikes, rhythmic slow wave (3 mo)	Intractable	−0.4 (4 mo)	Severe	Thin CC and hypoplasia of white matter, enlarged lateral ventricle (3 mo)
271	M	OS (→WS)	c.2627A>C, p.N876T, de novo	8 d	TS, eye deviation, mouth automatism	SB	Spasms (5 mo); hypsarrhythmia (5 mo); focal seizure (12 mo)	Intractable	−0.8 (2 mo)	Severe	Mild cerebral atrophy, delayed myelination (10 mo)
305	F	EOEE	c.787G>A, p.A263T, de novo	3 d	CS and TS	Multifocal spikes	Modified hypsarrhythmia (2 mo); mainly slow waves (10 mo)	Seizure-free after LTG at 6 mo	−0.1 (0 d)	Severe	Thin CC (2.5 mo)
322	M	OS (→WS)	c.2995G>A, p.E999K, N/A	6 d	CS	SB	Hypsarrhythmia (3 mo); spasms (4 mo)	Intractable	−0.6 (3 mo)	Severe	No abnormality (2 mo)

Abbreviations: CC = corpus callosum; CS = clonic seizure; DD = developmental delay; Dx = diagnosis; EOEE = early-onset epileptic encephalopathy; GTCS = generalized tonic-clonic seizure; HC-SD = head circumference SD; LEV = levetiracetam; LTG = lamotrigine; MISF = multiple independent spike foci; N/A = not available; OS = Ohtahara syndrome; PHT = phenytoin; SB = suppression-burst pattern; S-W = spike and slow wave; TS = tonic seizure; VGB = vigabatrin; WS = West syndrome; ZNS = zonisamide.

Figure 1 **Structure of the human $Na_v1.2$ channel with localization of *SCN2A* mutations**

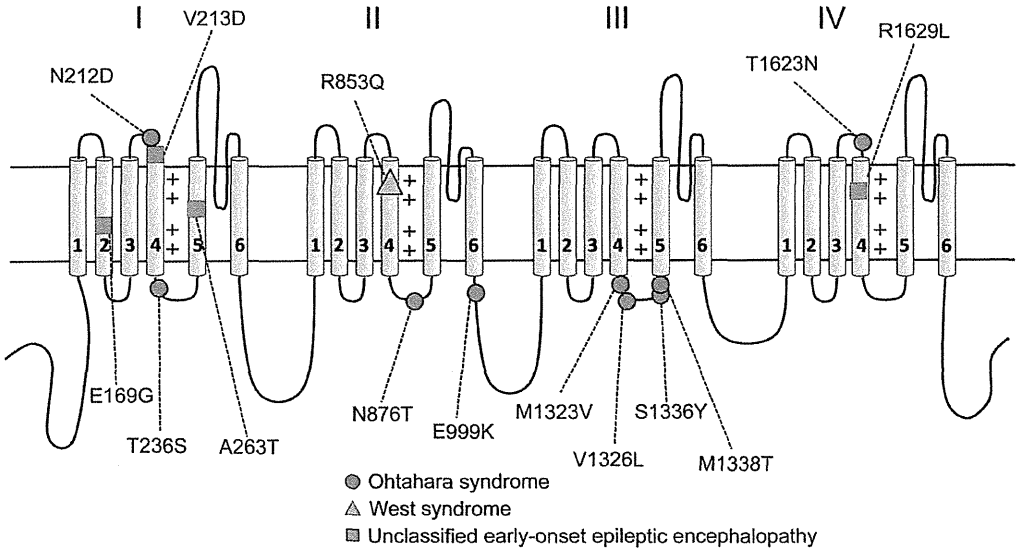

Red circles = Ohtahara syndrome; yellow triangle = West syndrome; blue squares = unclassified early-onset epileptic encephalopathy.

mutation in a patient with WS was located in a positively charged segment (S4) of domain II. Other mutations found in patients with unclassified EOEE were located in S4 of domain IV (1 mutation), a linker between S3 and S4 of domain I (1 mutation), and in S2 and S5 of domain I (2 mutations).

Clinical features of *SCN2A* mutations. The clinical information and EEG and MRI findings of patients with *SCN2A* mutations are summarized in table 1 and figure 2. Case reports (in appendix e-1) and further EEG (in figure e-2) and MRI (in figure e-3) findings are shown in supplemental data. There were 9 patients with OS (6 Japanese, 1 Canadian, 1 Mexican, and 1 Israeli), 1 with WS (Japanese), and 5 with unclassified EOEE (4 Japanese and 1 Slovenian). The ratio of females to males was 9:6. The mean age at onset was 45.3 days after birth (5.7 days in patients with OS; 65 days in unclassified EOEE; 10 months in a patient with WS). The initial epileptic attacks were tonic seizures in 8 patients, spasms in 3 patients, clonic seizures in 3 patients, and generalized tonic-clonic seizures in 1 patient. Three patients (patients 99, 254, and 305) had dystonia, and patient 99 also had chorea and ballismus. EEG at epilepsy onset showed suppression-burst pattern in 9 patients and focal or multifocal spikes in 6 patients. Seven of 15 patients with *SCN2A* mutations received adrenocorticotropic hormone therapy, leading to a transient reduction of seizures followed by recurrence. Epileptic seizures disappeared and EEG findings improved in 2 patients with WS and unclassified EOEE after administration of lamotrigine (patients 99 and 305), and in 1 patient with OS after combination therapy with zonisamide, levetiracetam, phenytoin, and vigabatrin (patient 146). Twelve of the 15 patients could not be controlled with antiepileptic drugs. All 15 patients had severe developmental delay, and 1 patient with unclassified EOEE (patient 185) died at the age of 5 years. Brain MRI showed cerebral atrophy in 10 patients, thin corpus callosum in 7 patients, delayed myelination in 5 patients, and cerebellar atrophy in 3 patients. MRI was normal in 2 patients in the early infantile period (1 and 2 months of age). Of the 9 patients with OS, 6 showed spasms, and all patients showed suppression-burst pattern on EEG at epilepsy onset. Seven patients with OS developed WS, and 1 case (patient 230) was suspected to do so because of spasms and developmental delay; however, no EEG was done to verify this.

DISCUSSION We identified 14 novel *SCN2A* mutations in 15 patients with EOEE. Two of the mutations could not be confirmed as de novo, but all mutations showed high scores for predicted negative effects on protein function, and were not found in our in-house control exome data. Of note, 9 of the 15 patients were diagnosed with OS, and all patients showed severe developmental delay. Previously, *SCN2A* mutations have been reported in a wide spectrum of disorders, including autism, severe nonsyndromic sporadic intellectual disability, benign seizure syndromes such as BFNIS, benign familial infantile seizure, and generalized epilepsy with febrile seizures plus, and severe epileptic disorders such as DS, infantile spasms, and AERRPS (acute encephalitis with refractory, repetitive partial seizures).[18–22,26–33]

Most of the disorders caused by *SCN1A* mutations involve DS or generalized epilepsy with febrile seizures

Figure 2 **EEG and brain MRI of patients with *SCN2A* mutations**

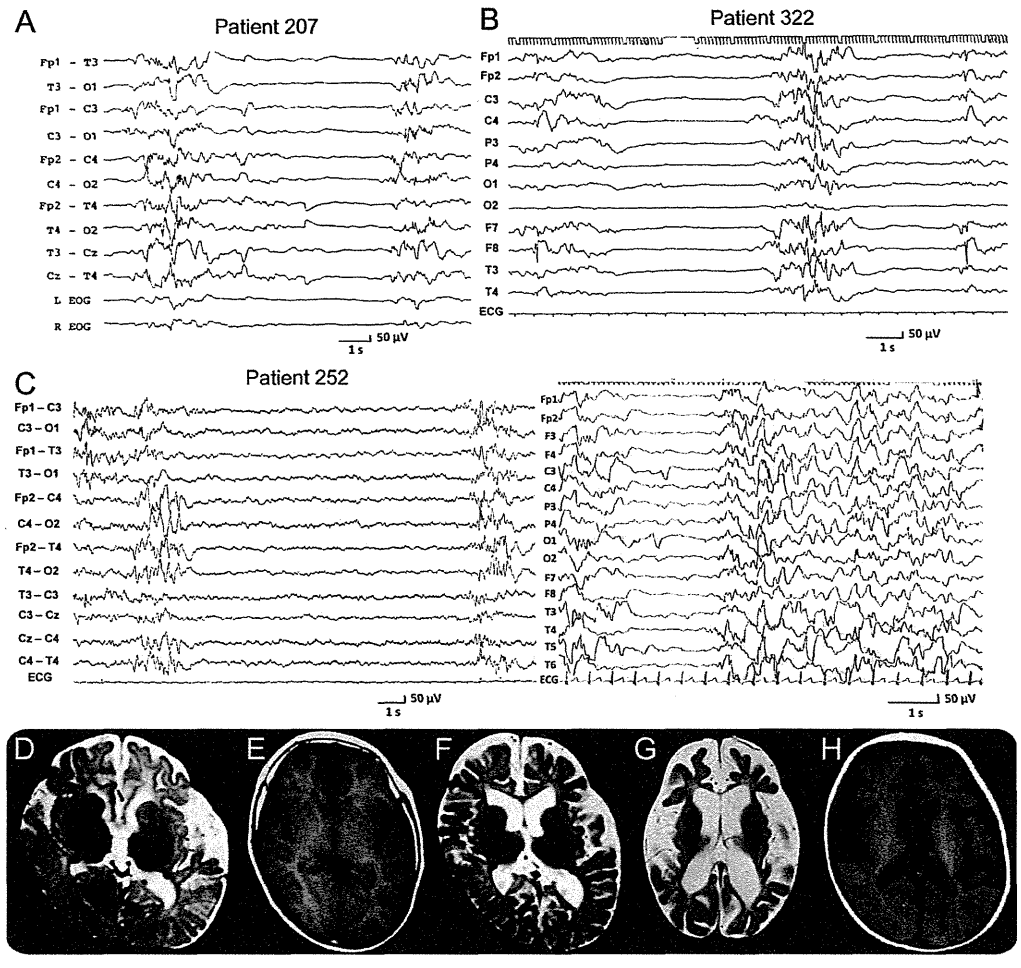

(A, B) Suppression-burst pattern on interictal EEG (A, patient 207 at an age of 18 days; B, patient 322 at an age of 7 days). (C) Suppression-burst pattern on interictal EEG of patient 252 at an age of 14 days (left). Transition from Ohtahara syndrome to West syndrome with modified hypsarrhythmia at an age of 3 months (right). (D–H) Brain MRI axial images at the level of the basal ganglia (D, T2-weighted image of patient 10 at 2 years and 2 months; E, T1-weighted image of patient 207 at 7 years; F, T2-weighted image of patient 251 at 1 year; G, T2-weighted image of patient 252 at 10 months; H, T1-weighted image of patient 271 at 10 months) showing cortical atrophy and delayed myelination (D, F–H) and cortical atrophy of the left temporal region (E).

plus, and onset of DS is usually in the infantile period.[17] By contrast, the onset of OS is neonatal and that of BFNIS is neonatal or early infantile. The phenotypic differences between *SCN2A* and *SCN1A* mutations might be explained by the different expression patterns of the channels. $Na_v1.2$ (SCN2A) and $Na_v1.6$ (SCN8A) are the major sodium channel α subunits in excitatory neurons. $Na_v1.2$ channels are expressed early in development and $Na_v1.6$ channels gradually replace $Na_v1.2$ channels in a population of neurons during maturation.[31] $Na_v1.2$ is expressed predominantly at terminals, unmyelinated axons, and in proximal axon initial segments, where action potentials are initiated, whereas $Na_v1.1$ (SCN1A) is expressed predominantly in neurons releasing γ-aminobutyric acid, and is localized to the soma and proximal processes of the neuron.[13,14,34,35] Therefore, *SCN1A* mutations may mainly lead to a reduction of sodium-channel activity in inhibitory neurons, increasing net excitability. However, *SCN2A* mutations likely also affect excitatory neurons and proximal axon initial segments especially during the early developmental period. Therefore, the effect of *SCN2A* mutations on the net excitability of neurons may result in earlier onset of epileptic disorders.

Investigation of the genotype-phenotype correlation of *SCN2A* mutations may contribute to our understanding of the pathophysiologic mechanisms of seizures caused by *SCN2A* mutations. *SCN2A* mutations causing BFNIS tend to be located in transmembrane regions (7/11 mutations), whereas mutations causing intractable epilepsies were located outside transmembrane domains, such as upstream of domain

I or between 2 domains.[18,19,21,26,28] In this study, all 9 mutations causing OS were found in linkers between transmembrane regions of $Na_v1.2$, especially between S4 and S5 of domain III. The S4-S5 linker of domain III interacts with the linker of domains III and IV, which is critical for fast inactivation of the sodium channel,[12,36] suggesting that alteration of this linker region may specifically affect the function of $Na_v1.2$. Similarly, the mutation causing WS was located in a positively charged segment (S4) of domain II, where no mutations have been previously reported. Interestingly, patient 10 showing OS had a low-level mosaicism of the p.V1326L mutation, which was confirmed in DNA samples from blood leukocytes, hair follicle, nail, and saliva. There are no previous reports of mosaicism for *SCN2A* mutations, but one case of mosaic 2q24 duplication including *SCN2A* and *SCN3A* has been reported.[37] The mosaic duplication was detected in 40% to 51% of blood cells, and the phenotype partially overlapped with both DS and BFNIS.[37] In cases of *SCN1A* mutations in familial DS, mosaic carriers with approximately 25% mutated alleles had experienced simple febrile seizure, whereas a carrier with approximately 12.5% mutated alleles was asymptomatic.[38] Patient 10 showed a very severe OS phenotype despite the low rate of mosaicism (18%). However, we did not determine whether the same mosaic rate was maintained in brain tissue. The location of the p.V1326L mutation in a linker of S4 and S5 of domain III might support the hypothesis that alteration of linker regions, especially between S4 and S5 of domain III, uniquely affects the function of $Na_v1.2$ in association with OS.

Patient 252 with OS had a de novo mutation in exon 6N, which is a neonatal isoform (transcript of variant 3). *SCN1A*, *SCN2A*, *SCN3A*, and *SCN8A* are subject to alternative splicing of exon 6N and 6A. In the developing mouse brain, *Scn2a* shows higher or equal amounts of the 6N isoform compared with the 6A isoform at birth, but 6N is gradually replaced by 6A during postnatal development.[39] The channels of the neonatal isoform are less excitable than the adult isoform.[40] In patient 252, the age of seizure onset was 14 days, which was relatively late compared with the other cases of OS. The expression of abnormal neonatal isoforms would be expected to gradually decrease, leading to an alleviation of neuronal hyperexcitability. In contrast, his symptoms, such as the transition to WS, development delay, and cerebral atrophy, worsened with increasing age. Further studies are required to clarify how mutations of the 6N isoform are involved in pathogenesis of EOEE.

To date, many disease-causing genes contributing to EOEE phenotypes have been identified, including *ARX*, *CDKL5*, *STXBP1*, *SPTAN1*, *KCNQ2*, *SCN1A*, and *SCN2A*.[5–11,17,20,21] In addition, mutations in one gene can cause a wide phenotypic spectrum as revealed by previous reports and the results of this study.[6,7,25] Therefore, rapid genetic diagnosis of EOEEs by screening for all known disease-causing genes with Sanger sequencing is very difficult. Recently, targeted exome sequencing has been developed and applied as a diagnostic tool for epileptic disorders.[33] Targeted exome sequencing as well as WES would be quite useful for genetic testing for EOEEs.

AUTHOR CONTRIBUTIONS

Kazuyuki Nakamura and Mitsuhiro Kato: study concept and design, analysis of the clinical data, interpretation of the data, and drafting/revising of the manuscript. Hitoshi Osaka, Sumimasa Yamashita, Eiji Nakagawa, Kazuhiro Haginoya, Jun Tohyama, Mitsuko Okuda, Takahito Wada, Shuichi Shimakawa, Katsumi Imai, Saoko Takeshita, Hisako Ishiwata, Dorit Lev, Tally Lerman-Sagie, David E. Cervantes-Barragán, Camilo E. Villarroel, Masaharu Ohfu, Karin Writzl, Barbara Gnidovec Stražišar, Shinichi Hirabayashi, David Chitayat, and Diane Myles Reid: analysis of the clinical data and sample collection. Kiyomi Nishiyama, Hirofumi Kodera, Mitsuko Nakashima, Yoshinori Tsurusaki, and Noriko Miyake: analysis of the genetic data. Kiyoshi Hayasaka: analysis of the clinical data and sample collection. Naomichi Matsumoto: study concept and design, interpretation of the data, and drafting/revising of the manuscript. Hirotomo Saitsu: study concept and design, analysis of the genetic data, interpretation of the data, and drafting/revising of the manuscript.

ACKNOWLEDGMENT

The authors thank the patients and their families for their participation in this study, and Aya Narita for her technical assistance.

STUDY FUNDING

Supported by the Ministry of Health, Labour and Welfare of Japan (24133701, 11103577, 11103340, 10103235), a Grant-in-Aid for Scientific Research (C) from the Japan Society for the Promotion of Science (24591500), a Grant-in-Aid for Young Scientists from the Japan Society for the Promotion of Science (10013428, 12020465), the Takeda Science Foundation, the Japan Science and Technology Agency, the Strategic Research Program for Brain Sciences (11105137), and a Grant-in-Aid for Scientific Research on Innovative Areas (Transcription Cycle) from the Ministry of Education, Culture, Sports, Science and Technology of Japan (12024421).

DISCLOSURE

K. Nakamura, M. Kato, H. Osaka, S. Yamashita, E. Nakagawa, and K. Haginoya report no disclosures. J. Tohyama is an investigator in clinical trials sponsored by Meiji Seika Pharma Co. Ltd., Novartis Pharma K.K., and UCB Japan Co. Ltd. M. Okuda, T. Wada, S. Shimakawa, K. Imai, S. Takeshita, H. Ishiwata, D. Lev, T. Lerman-Sagie, D. Cervantes-Barragán, C. Villarroel, M. Ohfu, K. Writzl, B. Gnidovec Stražišar, S. Hirabayashi, D. Chitayat, D. Myles Reid, K. Nishiyama, H. Kodera, M. Nakashima, and Y. Tsurusaki report no disclosures. N. Miyake is funded by research grants from the Ministry of Health, Labour and Welfare of Japan, a Grant-in-Aid for Young Scientists from the Japan Society for the Promotion of Science, and a Research Grant from the Takeda Science Foundation. K. Hayasaka reports no disclosures. N. Matsumoto is supported by grants from the Ministry of Health, Labour and Welfare of Japan, a Grant-in-Aid for Scientific Research (A) from the Japan Society for the Promotion of Science, the Takeda Science Foundation, the Japan Science and Technology Agency, the Strategic Research Program for Brain Sciences, a Grant-in-Aid for Scientific Research on Innovative Areas (Transcription Cycle) from the Ministry of Education, Culture, Sports, Science and Technology of Japan. H. Saitsu is funded by research grants from the Ministry of Health, Labour and Welfare of Japan, and a Grant-in-Aid for Young Scientists from the Japan Society for the Promotion of Science. Go to Neurology.org for full disclosures.

Received March 14, 2013. Accepted in final form June 6, 2013.

REFERENCES

1. Berg AT, Berkovic SF, Brodie MJ, et al. Revised terminology and concepts for organization of seizures and epilepsies: report of the ILAE Commission on Classification and Terminology, 2005–2009. Epilepsia 2010;51:676–685.
2. Mastrangelo M, Leuzzi V. Genes of early-onset epileptic encephalopathies: from genotype to phenotype. Pediatr Neurol 2012;46:24–31.
3. Ohtahara S, Yamatogi Y. Ohtahara syndrome: with special reference to its developmental aspects for differentiating from early myoclonic encephalopathy. Epilepsy Res 2006;70(suppl 1):S58–S67.
4. Kato M. A new paradigm for West syndrome based on molecular and cell biology. Epilepsy Res 2006;70(suppl 1):S87–S95.
5. Saitsu H, Kato M, Mizuguchi T, et al. De novo mutations in the gene encoding STXBP1 (MUNC18-1) cause early infantile epileptic encephalopathy. Nat Genet 2008;40:782–788.
6. Weckhuysen S, Mandelstam S, Suls A, et al. *KCNQ2* encephalopathy: emerging phenotype of a neonatal epileptic encephalopathy. Ann Neurol 2012;71:15–25.
7. Saitsu H, Kato M, Koide A, et al. Whole exome sequencing identifies *KCNQ2* mutations in Ohtahara syndrome. Ann Neurol 2012;72:298–300.
8. Weaving LS, Christodoulou J, Williamson SL, et al. Mutations of *CDKL5* cause a severe neurodevelopmental disorder with infantile spasms and mental retardation. Am J Hum Genet 2004;75;1079–1093.
9. Kato M, Saitoh S, Kamei A, et al. A longer polyalanine expansion mutation in the *ARX* gene causes early infantile epileptic encephalopathy with suppression-burst pattern (Ohtahara syndrome). Am J Hum Genet 2007;81:361–366.
10. Kato M, Das S, Petras K, Sawaishi Y, Dobyns WB. Polyalanine expansion of *ARX* associated with cryptogenic West syndrome. Neurology 2003;61:267–276.
11. Saitsu H, Tohyama J, Kumada T, et al. Dominant-negative mutations in alpha-II spectrin cause West syndrome with severe cerebral hypomyelination, spastic quadriplegia, and developmental delay. Am J Hum Genet 2010;86:881–891.
12. Catterall WA. From ionic currents to molecular mechanisms: the structure and function of voltage-gated sodium channels. Neuron 2000;26:13–25.
13. Whitaker WR, Faull RL, Waldvogel HJ, Plumpton CJ, Emson PC, Clare JJ. Comparative distribution of voltage-gated sodium channel proteins in human brain. Brain Res Mol Brain Res 2001;88:37–53.
14. Oliva M, Berkovic SF, Petrou S. Sodium channels and the neurobiology of epilepsy. Epilepsia 2012;53:1849–1859.
15. Zuberi SM, Brunklaus A, Birch R, Reavey E, Duncan J, Forbes GH. Genotype-phenotype associations in *SCN1A*-related epilepsies. Neurology 2011;76:594–600.
16. O'Roak BJ, Vives L, Girirajan S, et al. Sporadic autism exomes reveal a highly interconnected protein network of de novo mutations. Nature 2012;485:246–250.
17. Guerrini R. Dravet syndrome: the main issues. Eur J Paediatr Neurol 2012;16(suppl 1):S1–S4.
18. Heron SE, Crossland KM, Andermann E, et al. Sodium-channel defects in benign familial neonatal-infantile seizures. Lancet 2002;360:851–852.
19. Kamiya K, Kaneda M, Sugawara T, et al. A nonsense mutation of the sodium channel gene *SCN2A* in a patient with intractable epilepsy and mental decline. J Neurosci 2004;24:2690–2698.
20. Shi X, Yasumoto S, Nakagawa E, Fukasawa T, Uchiya S, Hirose S. Missense mutation of the sodium channel gene *SCN2A* causes Dravet syndrome. Brain Dev 2009;31:758–762.
21. Ogiwara I, Ito K, Sawaishi Y, et al. De novo mutations of voltage-gated sodium channel alphaII gene *SCN2A* in intractable epilepsies. Neurology 2009;73:1046–1053.
22. Kobayashi K, Ohzono H, Shinohara M, et al. Acute encephalopathy with a novel point mutation in the *SCN2A* gene. Epilepsy Res 2012;102:109–112.
23. DePristo MA, Banks E, Poplin R, et al. A framework for variation discovery and genotyping using next-generation DNA sequencing data. Nat Genet 2011;43:491–498.
24. Wang K, Li M, Hakonarson H. ANNOVAR: functional annotation of genetic variants from high-throughput sequencing data. Nucleic Acids Res 2010;38:e164.
25. Saitsu H, Kato M, Osaka H, et al. *CASK* aberrations in male patients with Ohtahara syndrome and cerebellar hypoplasia. Epilepsia 2012;53:1441–1449.
26. Herlenius E, Heron SE, Grinton BE, et al. *SCN2A* mutations and benign familial neonatal-infantile seizures: the phenotypic spectrum. Epilepsia 2007;48:1138–1142.
27. Sugawara T, Tsurubuchi Y, Agarwala KL, et al. A missense mutation of the Na^+ channel alpha II subunit gene Na(v)1.2 in a patient with febrile and afebrile seizures causes channel dysfunction. Proc Natl Acad Sci USA 2001;98:6384–6389.
28. Berkovic SF, Heron SE, Giordano L, et al. Benign familial neonatal-infantile seizures: characterization of a new sodium channelopathy. Ann Neurol 2004;55:550–557.
29. Ito M, Shirasaka Y, Hirose S, Sugawara T, Yamakawa K. Seizure phenotypes of a family with missense mutations in *SCN2A*. Pediatr Neurol 2004;31:150–152.
30. Striano P, Bordo L, Lispi ML, et al. A novel *SCN2A* mutation in family with benign familial infantile seizures. Epilepsia 2006;47:218–220.
31. Liao Y, Deprez L, Maljevic S, et al. Molecular correlates of age-dependent seizures in an inherited neonatal-infantile epilepsy. Brain 2010;133:1403–1414.
32. Need AC, Shashi V, Hitomi Y, et al. Clinical application of exome sequencing in undiagnosed genetic conditions. J Med Genet 2012;49:353–361.
33. Lemke JR, Riesch E, Scheurenbrand T, et al. Targeted next generation sequencing as a diagnostic tool in epileptic disorders. Epilepsia 2012;53:1387–1398.
34. Furuyama T, Morita Y, Inagaki S, Takagi H. Distribution of I, II and III subtypes of voltage-sensitive Na^+ channel mRNA in the rat brain. Brain Res Mol Brain Res 1993;17:169–173.
35. Ogiwara I, Miyamoto H, Morita N, et al. Nav1.1 localizes to axons of parvalbumin-positive inhibitory interneurons: a circuit basis for epileptic seizures in mice carrying an *Scn1a* gene mutation. J Neurosci 2007;27:5903–5914.
36. Smith MR, Goldin AL. Interaction between the sodium channel inactivation linker and domain III S4-S5. Biophys J 1997;73:1885–1895.
37. Vecchi M, Cassina M, Casarin A, et al. Infantile epilepsy associated with mosaic 2q24 duplication including *SCN2A* and *SCN3A*. Seizure 2011;20:813–816.
38. Shi YW, Yu MJ, Long YS, et al. Mosaic *SCN1A* mutations in familial partial epilepsy with antecedent febrile seizures. Genes Brain Behav 2012;11:170–176.
39. Gazina EV, Richards KL, Mokhtar MB, Thomas EA, Reid CA, Petrou S. Differential expression of exon 5 splice variants of sodium channel alpha subunit mRNAs in the developing mouse brain. Neuroscience 2010;166:195–200.
40. Xu R, Thomas EA, Jenkins M, et al. A childhood epilepsy mutation reveals a role for developmentally regulated splicing of a sodium channel. Mol Cell Neurosci 2007;35:292–301.

CLINICAL REPORT

AMERICAN JOURNAL OF medical genetics A

Co-Occurrence of 22q11 Deletion Syndrome and HDR Syndrome

Ryoko Fukai,[1,2] Nobuhiko Ochi,[3] Akira Murakami,[1] Mitsuko Nakashima,[1] Yoshinori Tsurusaki,[1] Hirotomo Saitsu,[1] Naomichi Matsumoto,[1]* and Noriko Miyake[1]*

[1]Department of Human Genetics, Yokohama City University, Graduate School of Medicine, Yokohama, Japan

[2]Department of Neurology and Stroke Medicine, Yokohama City University Graduate School of Medicine, Yokohama, Japan

[3]Department of Pediatrics, Aichi Prefectural Hospital and Rehabilitation Center for Disabled Children, Dai-ni Aoitori Gakuen, Okazaki, Japan

Manuscript Received: 23 November 2012; Manuscript Accepted: 16 May 2013

22q11 deletion syndrome is one of the most common chromosomal deletion syndromes and is usually caused by a 1.5–3.0 Mb deletion at chromosome 22q11.2. It is characterized by hypocalcemia resulting from hypoplasia of the parathyroid glands, hypoplasia of the thymus, and defects of the cardiac outflow tract. We encountered a Japanese boy presenting with an unusually severe phenotype of 22q11 deletion syndrome, including progressive renal failure and severe intellectual disabilities. Diagnostic testing using fluorescent in situ hybridization revealed deletion of the 22q11 region, but this did not explain the additional complications. Copy number analysis was therefore performed using whole genome single nucleotide polymorphism (SNP) assay, which identified an additional de novo deletion at 10p14. This region is the locus for hypoparathyroidism, deafness, and renal dysplasia (HDR) syndrome caused by haploinsufficiency of *GATA3*. Together, these two syndromes sufficiently explain the patient's phenotype. This is the first known case report of the co-occurrence of 22q11 deletion syndrome and HDR syndrome. As the two syndromes overlap clinically, this study indicates the importance of carrying out careful clinical and genetic assessment of patients with atypical clinical phenotypes or unique complications. Unbiased genetic analysis using whole genome copy number SNP arrays is especially useful for detecting such rare double mutations.

Key words: whole genome SNP assay; 22q11 deletion syndrome; HDR syndrome; double mutations; FISH

How to Cite this Article:
Fukai R, Ochi N, Murakami A, Nakashima M, Tsurusaki Y, Saitsu H, Matsumoto N, Miyake N. 2013. Co-occurrence of 22q11 deletion syndrome and HDR syndrome.
Am J Med Genet Part A 161A:2576–2581.

INTRODUCTION

22q11 deletion syndrome is caused by a 1.5–3.0 Mb deletion of chromosome 22q11.2. It is clinically characterized by developmental delay, facial dysmorphism, congenital heart defects, hypoplasia of the thymus, immunodeficiency, aplasia or hypoplasia of the parathyroid glands, and tapered fingers [Perez and Sullivan, 2002; Digilio et al., 2005; Goldmuntz, 2005; Kobrynski and Sullivan, 2007; McDonald-McGinn and Sullivan, 2011]. 22q11 deletion syndrome is the most common chromosomal deletion syndrome with an estimated incidence of 1/4,000 live births [Kitsiou-Tzeli et al., 2004; Kobrynski and Sullivan, 2007; McDonald-McGinn and Sullivan, 2011; Gennery, 2012].

The region 10p13-p14 is known as the second DiGeorge syndrome (DGS) critical region (DGCR2) [Lichtner et al., 2000], and deletions of DGCR2 cause hypoparathyroidism with sensorineural deafness and renal dysplasia (HDR) syndrome [OMIM #146255]. Haploinsufficiency of *GATA3* (NM_001002295) at 10p14 is causative for HDR. HDR is a rare syndrome, with around 50 reported patients [Greenberg et al., 1986; Shapira et al., 1994; Gottlieb et al., 1998; Schuffenhauer et al., 1998; Lichtner et al., 2000; Van

Conflict of interest: none.
Grant sponsor: Ministry of Health, Labour and Welfare; Grant sponsor: Japan Science and Technology Agency; Grant sponsor: Japan Society for the Promotion of Science; Grant sponsor: Strategic Research Promotion of Yokohama City University; Grant sponsor: Japan Epilepsy Research Foundation; Grant sponsor: Naito Foundation; Grant sponsor: Takeda Science Foundation; Grant sponsor: Yokohama Foundation for Advancement of Medical Science; Grant sponsor: Hayashi Memorial Foundation for Female Natural Scientists.
*Correspondence to:
Noriko Miyake, M.D., Ph.D. and Naomichi Matsumoto, M.D., Ph.D., Department of Human Genetics, Yokohama City University, Graduate School of Medicine, 3-9 Fukuura, Kanazawa-Ku, Yokohama 236-0004, Japan.
E-mail: nmiyake@yokohama-cu.ac.jp (N. Miyake), naomat@yokohama-cu.ac.jp (N. Matsumoto)
Article first published online in Wiley Online Library (wileyonlinelibrary.com): 5 August 2013
DOI 10.1002/ajmg.a.36083

Esch et al., 2000; Muroya et al., 2001; Skrypnyk et al., 2002; Yatsenko et al., 2004; Mino et al., 2005; Zahirieh et al., 2005; Thakker, 2008; Benetti et al., 2009; Lindstrand et al., 2010; Fukami et al., 2011].

Here, we present the case of a Japanese boy with 22q11 deletion syndrome and HDR syndrome, which were confirmed by whole genome microarray.

PATIENT AND METHODS

Clinical Report

The patient is a 22-year-old male who was the first child born to healthy, nonconsanguineous Japanese parents. After a normal pregnancy, he was born at 37 weeks of gestation. His birth weight was 2,412 g (−1.4 SD), length 45 cm (−1.9 SD), and his occipital-frontal circumference (OFC) was 31.5 cm (−1.3 SD). The patient's facial features (hooded eyelid, bulbous nasal tip, low-set posteriorly rotated ears, and small mouth), cleft palate, umbilical hernia, inguinal hernia, and tapered fingers implied the presence of a congenital syndrome (Fig. 1). At 6 months of age, his length was 61.6 cm (−2.5 SD), weight 6,000 g (−2.2 SD), and OFC 43 cm (−0.23 SD). At 1 year his length was 73 cm (−0.77 SD), weight 7,850 g (−1.57 SD), and OFC 46.5 cm (+0.28 SD). At 5 years and 1 month his height was 93.1 cm (−3.2 SD) and weight 12.5 kg (−2.0 SD), and at 13 years and 9 months his height was 130 cm (−3.8 SD) and weight 27 kg (−2.2 SD).

He showed developmental delay, achieving head control at 6 months of age, sitting at 15 months, and walking at 2 years and 9 months. He developed convulsions at the age of 5 months, and was treated with phenobarbital and clonazepam based on a diagnosis of West syndrome. The convulsions disappeared following treatment at the age of three and a half years, but relapsed at the age of nine and became uncontrollable at age 21. At 6 months, severe sensorineural hearing loss was noted with an auditory brainstem response score of >90 dB. At the age of one, signs of autism were observed including a lack of eye contact, no interest in people including his parents, no interest in toys, and unusual repetitive movements such as lifting and shaking his hands. He has uttered words, but these have never been meaningful. At the age of three, his hyperkinesis and autistic behaviors were more obvious and he was diagnosed as autistic according to The Diagnostic and Statistical Manual of Mental Disorders IV criteria. His psychomotor delay was profound (I.Q. <20). At the age of nine, additional autistic repetitive behaviors, such as wandering around alone and covering his ears, and impulsive movements, such as ascending to high altitudes, were observed. However, this behavior was controlled by the age of 18 following the oral administration of risperidone.

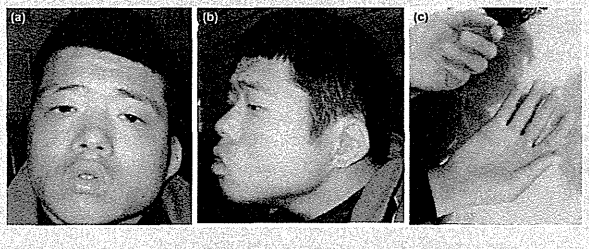

FIG. 1. Clinical features of the patient. Photographs of the patient at 22 years of age showing facial features, small mouth, low-set ears (a,b) and tapered fingers (c).

A peripheral blood examination performed at the age of three indicated kidney dysfunction (creatinine, 1.0 mg/dl (normal range: 0.3–0.5 mg/dl), blood urea nitrogen (BUN), 65 mg/dl (normal range: 5–18 mg/dl)). He exhibited tubular damage and his renal function deteriorated until his right kidney and urinary tract were undetectable by intravenous pyelogram at the age of 10. Hypocalcemia (Ca, 5.2 mg/dl; normal range: 9.6–11.6 mg/dl) was first detected at 5 months of age, when an oral supplement of calcium and vitamin D analog (alfacalcidol) were prescribed. However, despite the supplements, hypocalcemia (Ca, 6.4 mg/dl; normal range: 8.5–10.2 mg/dl) and low serum high sensitive parathyroid hormone (HSPTH) levels (<100 mg/ml; normal range: 160–520 mg/ml) remained at the age of 10.

Genomic DNA Preparation

Peripheral blood samples from the patient's family (the patient and his parents) were collected with informed consent. Genomic DNA was extracted using the QuickGene DNA whole blood kit L (Fujifilm, Tokyo, Japan). This study was approved by the Institutional Review Board for Ethical Issues at Yokohama City University School of Medicine, Yokohama, Japan.

Copy Number Variation Detection

Copy number variations (CNVs) were analyzed using Affymetrix Cytogenetics Whole-Genome 2.7M Array (Affymetrix, Santa Clara, CA, USA) according to the manufacturer's instructions. CNVs were analyzed by Chromosome Analysis Suite (ChAS) v1.2 software (Affymetrix) with NA32 (hg19) annotations. The detection conditions for ChAS were set as follows: a confidence value of 90%, 20 contiguous probes, and larger than 100 kb for duplications; and a confidence value of 89%, 20 contiguous markers, and larger than 10 kb for deletions.

Fluorescence In Situ Hybridization (FISH)

Fluorescence in situ hybridization (FISH) was performed on fixed peripheral lymphocytes as previously reported [Nishimura-Tadaki et al., 2011]. Four RPCI-11 human bacterial artificial chromosome clones were used: RP11-91K20 (chr10:8,303,515-8,458,288 bp) and RP11-1057H19 (chr22:19,310,701-19,484,643 bp) for the deleted region, and RP11-1069N9 (chr10:90,801-288,527 bp) and RP11-81N15 (chr22:42,605,111-42,773,705 bp) for references.

RESULTS

22q11 deletion syndrome was suspected based on the patient's clinical features, and FISH confirmed the presence of the 22q11.2 deletion. However, the severe renal failure, persistent hypocalcemia, and intractable epilepsy seemed atypical for 22q11 deletion

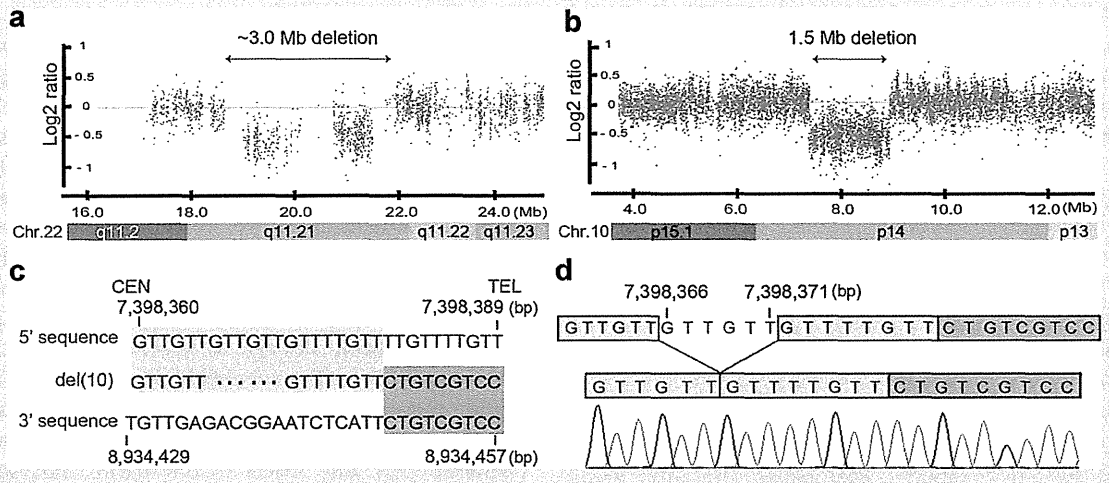

FIG. 2. Cytogenetic and molecular analyses of two deleted regions. a,b: Array plots showing the deletion at 22q11.21 (a) and 10p14 (b). c: Sequencing analysis of the breakpoint of the 10p14 deletion. Upper and lower sequences are references adjacent to the proximal and distal deletion breakpoints, respectively. Middle sequence shows the deletion junction in the patient. Light and dark gray boxes show sequence homology with the upper and lower references, respectively. Black dots indicate 6-bp deletion. d: Electropherogram of the breakpoint and 6-bp deletion.

syndrome. Thus, we performed high-resolution copy number analysis to investigate additional genetic change(s) to explain the atypical clinical presentation.

Whole genome single nucleotide polymorphism (SNP) array identified two pathological deletions at 22q11.2 (19.0-22.0 Mb; Fig. 2a) and 10p14 (7.4–8.9 Mb; Fig. 2b). The deletion at 10p14 spanned 1.5 Mb, and included eight known genes. One of these was *GATA3*, which is mutated in HDR syndrome. Both of these deletions occurred de novo, as confirmed by FISH (Fig. 3). Sequencing analysis of the 10p14 deletion breakpoint showed it to be from 7,398,380 to 8,934,448 bp, together with a GTTGTT deletion from 7,398,366 to 7,398,371 bp (Fig. 2c and d).

DISCUSSION

In this report, we describe a unique patient with two de novo deletions at 22q11.2 and 10p14. He was initially diagnosed with 22q11 deletion syndrome, but his severe and atypical features

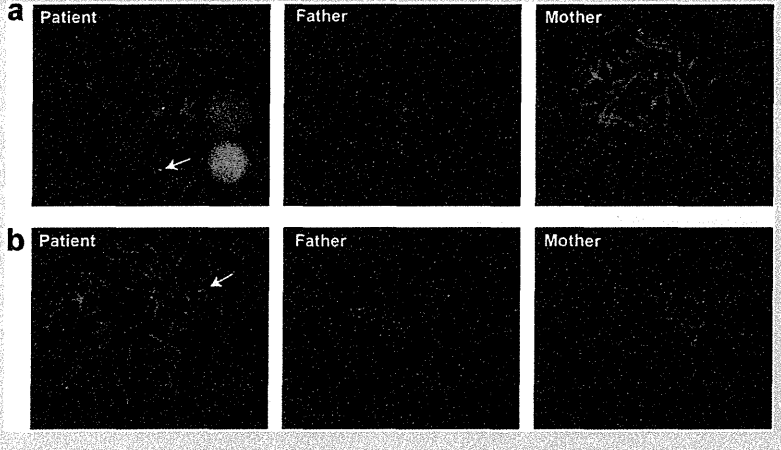

FIG. 3. Two de novo deletions shown by FISH analysis. Two-color FISH images illustrating a de novo deletion at 22q11.21 using probe RP11-1057H19 (red signals) for deletion and probe RP11-81N15 (green signals) for reference (a), and a de novo deletion at 10p14 using probe RP11-1069N9 (green signals) for deletion and probe RP11-91K20 (red signals) for reference (b). White arrows indicate a loss of signal.

(severe hypocalcemia and progressive renal failure) implied the possible involvement of other genetic changes. Driven by this hypothesis, we identified a 10p14 causative deletion for HDR syndrome in addition to the 22q11.2 deletion.

Highly variable clinical features of 22q11 deletion syndrome are well recognized [Swillen et al., 2000; McDonald-McGinn and Sullivan, 2011], although the mechanism behind this phenotype variation remains unclear. It could be partially explained by differences in deleted regions, additional genomic factors such as copy number variation and/or the unmasking of autosomal recessive conditions [Girirajan et al., 2012; Li et al., 2012].

Haploinsufficiencies of *GATA3* and *TBX1* are known to be responsible for the major clinical manifestations of HDR syndrome and 22q11 deletion syndrome, respectively [Van Esch et al., 2000; Lindsay et al., 2001; Merscher et al., 2001]. *GATA3* is a zinc-finger transcription factor that is expressed in the central and peripheral nervous system, inner ear, thymus, parathyroid, liver, kidney, and hematopoietic cell lineage [Oosterwegel et al., 1992; Ting et al., 1996]. Similar to HDR syndrome in humans, *Gata3* null mice suffer from craniofacial malformations, neural tube defects, renal hypoplasia, and abnormal hematopoiesis. They usually die by embryonic Day 11–12 [Pandolfi et al., 1995; Lim et al., 2000].

TBX1 encodes a DNA binding transcription factor of the T-box family, which is expressed mainly in the cardiovascular system, thymus, and parathyroid gland [Chapman et al., 1996; Garg et al., 2001; Jerome and Papaioannou, 2001; Lindsay et al., 2001; Merscher et al., 2001; Yagi et al., 2003; Zahirieh et al., 2005]. Resembling 22q11 deletion syndrome in humans, heterozygous $Tbx1^{+/-}$ mice often show cardiac outflow tract anomalies, while *Tbx1* null mice present with a shortened neck, hypoplastic mandible, low-set ears, abnormal aortic arch, hypoplasia/aplasia of the thymus and parathyroid gland, and die at birth from respiratory failure [Jerome and Papaioannou, 2001]. While the organs of expression of these two genes and the clinical phenotypes are similar in humans and mice, no evidence of a direct or indirect functional relationship between *TBX1* and *GATA3* has been reported.

By contrast, *Gata3* is expressed both in the inner ear and auditory neurons [Karis et al., 2001], and *Gata3* heterozygous and null mice have innervation defects in their ears [Karis et al., 2001]. This is similar to the common HDR syndrome phenotype of sensorineural hearing loss. In addition, *Tbx1* is expressed in the first pharyngeal pouch and the otic vesicle, which form outer and inner ears [Lawoko-Kerali et al., 2004]. *Tbx1* null mice, but not heterozygous $Tbx1^{+/-}$ mice, show morphological defects of the ear [Arnold et al., 2006]. This is similar to the majority of patients with 22q11 deletion syndrome, who have conductive hearing loss caused by chronic otitis media as a result of structural abnormalities of the ear and/or immunological deficiencies. The differences of the expression pattern of TBX1 and GATA3 within the ear could explain the predominant type of hearing impairment: sensorineural in HDR syndrome and conductive hearing loss in 22q11 deletion syndrome.

TABLE I. Clinical Features of 22q11 Deletion Syndrome, HDR Syndrome, and the Proband

	22q11 deletion syndrome	HDRS		
Clinical features	**% (n = 906)**	**%**	**Number of patients**	**Proband**
Developmental delay	45	85.7	(18/21)	+
Intellectual disabilities	30	67.9	(19/28)	+
Motor function/hypotonia	NM	87.5	(7/8)	+
Dysmorphic features				
Hooded eyelid	25	NM	NM	+
Bulbous nasal tip	60	92.3	(12/13)	+
Cleft palate	27	16.7	(2/12)	+
Posteriorly rotated ears	13	92.3	(12/13)	+
Long tapered fingers	Most	NM	NM	+
Hearing loss				
Conductive	31	0	(0/30)	−
Sensorineural	2	93.3	(28/30)	+
Central nervous system				
Brain abnormalities	≦1	88.9	(8/9)	+
Seizures	Infrequent	63.0	(17/27)	+
ADHD	54	NM	NM	+
Autism	14	66.7	(2/3)	+
Hypocalcemia (hypoparathyroidism)	49	90.3	(28/31)	+
Immunodeficiency	77	15.4	(2/13)	−
Cardiac anomaly	77	27.3	(6/22)	−
Renal anomaly	36	69.7	(23/33)	+
Renal dysfunction	NM	33.3	(8/24)	+

The frequency of clinical features in 22q11 deletion syndrome was based on the previous report by McDonald-McGinn and Sullivan [2011]. The frequency of clinical features in HDRS was calculated from a series of references mentioned in the text. NM, not mentioned; +, presence of symptom; −, symptom not present.

While the overlapping features of the two syndromes in the present patient made it difficult to conclude which symptoms originated from each deletion (Table I), it can be supposed that the combined effects of two clinically similar syndromes would worsen the total symptoms. The additional disruptions may generate a more severe phenotype than the outcome from either the first or second hit by lowering the threshold for phenotypes as seen in previous studies [Girirajan and Eichler, 2010; Kumar, 2010].

In conclusion, the rare phenotypes of our patient enabled us to detect the co-occurrence of de novo 22q11.2 and 10p14 deletions. This study reaffirmed the importance of carrying out detailed clinical examinations and unbiased genetic analysis, particularly for patients presenting with atypical clinical phenotypes. In such instances, it would be beneficial to uncover all pathological alterations to understand the unresolved etiology of the phenotypes.

ACKNOWLEDGMENTS

We thank the patient and his family for participating in this work. We also thank Ms. Y. Yamashita and E. Koike for their technical assistance. This work was supported by Research Grants from the Ministry of Health, Labour and Welfare (N. Miyake, H.S., and N. Matsumoto), the Japan Science and Technology Agency (N. Matsumoto), a Grant-in-Aid for Scientific Research from the Japan Society for the Promotion of Science (N. Matsumoto), a Grant-in-Aid for Young Scientists from the Japan Society for the Promotion of Science (N. Miyake, H.S.), a Grant for 2012 Strategic Research Promotion of Yokohama City University (N. Matsumoto), Research Grants from the Japan Epilepsy Research Foundation (H.S.), the Naito Foundation (N. Matsumoto), the Takeda Science Foundation (N. Matsumoto and N. Miyake), the Yokohama Foundation for Advancement of Medical Science (N. Miyake), and the Hayashi Memorial Foundation for Female Natural Scientists (N. Miyake).

REFERENCES

Arnold JS, Braunstein EM, Ohyama T, Groves AK, Adams JC, Brown MC, Morrow BE. 2006. Tissue-specific roles of Tbx1 in the development of the outer, middle and inner ear, defective in 22q11DS patients. Hum Mol Genet 15:1629–1639.

Benetti E, Murer L, Bordugo A, Andreetta B, Artifoni L. 2009. 10p12.1 deletion: HDR phenotype without DGS2 features. Exp Mol Pathol 86:74–76.

Chapman DL, Garvey N, Hancock S, Alexiou M, Agulnik SI, Gibson-Brown JJ, Cebra-Thomas J, Bollag RJ, Silver LM, Papaioannou VE. 1996. Expression of the T-box family genes, Tbx1–Tbx5, during early mouse development. Dev Dyn 206:379–390.

Digilio M, Marino B, Capolino R, Dallapiccola B. 2005. Clinical manifestations of deletion 22q11.2 syndrome (DiGeorge/velo-cardio-facial syndrome). Images Paediatr Cardiol 7:23–34.

Fukami M, Muroya K, Miyake T, Iso M, Kato F, Yokoi H, Suzuki Y, Tsubouchi K, Nakagomi Y, Kikuchi N, Horikawa R, Ogata T. 2011. GATA3 abnormalities in six patients with HDR syndrome. Endocr J 58:117–121.

Garg V, Yamagishi C, Hu T, Kathiriya IS, Yamagishi H, Srivastava D. 2001. Tbx1, a DiGeorge syndrome candidate gene, is regulated by sonic hedgehog during pharyngeal arch development. Dev Biol 235:62–73.

Gennery AR. 2012. Immunological aspects of 22q11.2 deletion syndrome. Cell Mol Life Sci 69:17–27.

Girirajan S, Eichler EE. 2010. Phenotypic variability and genetic susceptibility to genomic disorders. Hum Mol Genet 19:R176–R187.

Girirajan S, Rosenfeld JA, Coe BP, Parikh S, Friedman N, Goldstein A, Filipink RA, McConnell JS, Angle B, Meschino WS, Nezarati MM, Asamoah A, Jackson KE, Gowans GC, Martin JA, Carmany EP, Stockton DW, Schnur RE, Penney LS, Martin DM, Raskin S, Leppig K, Thiese H, Smith R, Aberg E, Niyazov DM, Escobar LF, El-Khechen D, Johnson KD, Lebel RR, Siefkas K, Ball S, Shur N, McGuire M, Brasington CK, Spence JE, Martin LS, Clericuzio C, Ballif BC, Shaffer LG, Eichler EE. 2012. Phenotypic heterogeneity of genomic disorders and rare copy-number variants. N Engl J Med 367:1321–1331.

Goldmuntz E. 2005. DiGeorge syndrome: New insights. Clin Perinatol 32:963–978.

Gottlieb S, Driscoll DA, Punnett HH, Sellinger B, Emanuel BS, Budarf ML. 1998. Characterization of 10p deletions suggests two nonoverlapping regions contribute to the DiGeorge syndrome phenotype. Am J Hum Genet 62:495–498.

Greenberg F, Valdes C, Rosenblatt HM, Kirkland JL, Ledbetter DH. 1986. Hypoparathyroidism and T cell immune defect in a patient with 10p deletion syndrome. J Pediatr 109:489–492.

Jerome LA, Papaioannou VE. 2001. DiGeorge syndrome phenotype in mice mutant for the T-box gene, Tbx1. Nat Genet 27:286–291.

Karis A, Pata I, van Doorninck JH, Grosveld F, de Zeeuw CI, de Caprona D, Fritzsch B. 2001. Transcription factor GATA-3 alters pathway selection of olivocochlear neurons and affects morphogenesis of the ear. J Comp Neurol 429:615–630.

Kitsiou-Tzeli S, Kolialexi A, Fryssira H, Galla-Voumvouraki A, Salavoura K, Kanariou M, Tsangaris GT, Kanavakis E, Mavrou A. 2004. Detection of 22q11.2 deletion among 139 patients with Di George/velocardiofacial syndrome features. In Vivo 18:603–608.

Kobrynski LJ, Sullivan KE. 2007. Velocardiofacial syndrome, DiGeorge syndrome: The chromosome 22q11.2 deletion syndromes. Lancet 370:1443–1452.

Kumar RA. 2010. Two-hit wonder: A novel genetic model to explain variable expressivity in severe pediatric phenotypes. Clin Genet 78:517–519.

Lawoko-Kerali G, Rivolta MN, Lawlor P, Cacciabue-Rivolta DI, Langton-Hewer C, van Doorninck JH, Holley MC. 2004. GATA3 and NeuroD distinguish auditory and vestibular neurons during development of the mammalian inner ear. Mech Dev 121:287–299.

Li D, Tekin M, Buch M, Fan YS. 2012. Co-existence of other copy number variations with 22q11.2 deletion or duplication: A modifier for variable phenotypes of the syndrome? Mol Cytogenet 5:18.

Lichtner P, Konig R, Hasegawa T, Van Esch H, Meitinger T, Schuffenhauer S. 2000. An HDR (hypoparathyroidism, deafness, renal dysplasia) syndrome locus maps distal to the DiGeorge syndrome region on 10p13/14. J Med Genet 37:33–37.

Lim KC, Lakshmanan G, Crawford SE, Gu Y, Grosveld F, Engel JD. 2000. Gata3 loss leads to embryonic lethality due to noradrenaline deficiency of the sympathetic nervous system. Nat Genet 25:209–212.

Lindsay EA, Vitelli F, Su H, Morishima M, Huynh T, Pramparo T, Jurecic V, Ogunrinu G, Sutherland HF, Scambler PJ, Bradley A, Baldini A. 2001. Tbx1 haploinsufficiency in the DiGeorge syndrome region causes aortic arch defects in mice. Nature 410:97–101.

Lindstrand A, Malmgren H, Verri A, Benetti E, Eriksson M, Nordgren A, Anderlid BM, Golovleva I, Schoumans J, Blennow E. 2010. Molecular and clinical characterization of patients with overlapping 10p deletions. Am J Med Genet Part A 152A:1233–1243.

McDonald-McGinn DM, Sullivan KE. 2011. Chromosome 22q11.2 deletion syndrome (DiGeorge syndrome/velocardiofacial syndrome). Medicine 90:1–18.

Merscher S, Funke B, Epstein JA, Heyer J, Puech A, Lu MM, Xavier RJ, Demay MB, Russell RG, Factor S, Tokooya K, Jore BS, Lopez M, Pandita RK, Lia M, Carrion D, Xu H, Schorle H, Kobler JB, Scambler P, Wynshaw-Boris A, Skoultchi AI, Morrow BE, Kucherlapati R. 2001. TBX1 is responsible for cardiovascular defects in velo-cardio-facial/ DiGeorge syndrome. Cell 104:619–629.

Mino Y, Kuwahara T, Mannami T, Shioji K, Ono K, Iwai N. 2005. Identification of a novel insertion mutation in GATA3 with HDR syndrome. Clin Exp Nephrol 9:58–61.

Muroya K, Hasegawa T, Ito Y, Nagai T, Isotani H, Iwata Y, Yamamoto K, Fujimoto S, Seishu S, Fukushima Y, Hasegawa Y, Ogata T. 2001. GATA3 abnormalities and the phenotypic spectrum of HDR syndrome. J Med Genet 38:374–380.

Nishimura-Tadaki A, Wada T, Bano G, Gough K, Warner J, Kosho T, Ando N, Hamanoue H, Sakakibara H, Nishimura G, Tsurusaki Y, Doi H, Miyake N, Wakui K, Saitsu H, Fukushima Y, Hirahara F, Matsumoto N. 2011. Breakpoint determination of X;autosome balanced translocations in four patients with premature ovarian failure. J Hum Genet 56:156–160.

Oosterwegel M, Timmerman J, Leiden J, Clevers H. 1992. Expression of GATA-3 during lymphocyte differentiation and mouse embryogenesis. Dev Immunol 3:1–11.

Pandolfi PP, Roth ME, Karis A, Leonard MW, Dzierzak E, Grosveld FG, Engel JD, Lindenbaum MH. 1995. Targeted disruption of the GATA3 gene causes severe abnormalities in the nervous system and in fetal liver haematopoiesis. Nat Genet 11:40–44.

Perez E, Sullivan KE. 2002. Chromosome 22q11.2 deletion syndrome (DiGeorge and velocardiofacial syndromes). Curr Opin Pediatr 14:678–683.

Schuffenhauer S, Lichtner P, Peykar-Derakhshandeh P, Murken J, Haas OA, Back E, Wolff G, Zabel B, Barisic I, Rauch A, Borochowitz Z, Dallapiccola B, Ross M, Meitinger T. 1998. Deletion mapping on chromosome 10p and definition of a critical region for the second DiGeorge syndrome locus (DGS2). Eur J Hum Genet 6:213–225.

Shapira M, Borochowitz Z, Bar-El H, Dar H, Etzioni A, Lorber A. 1994. Deletion of the short arm of chromosome 10 (10p13): Report of a patient and review. Am J Med Genet 52:34–38.

Skrypnyk C, Goecke TO, Majewski F, Bartsch O. 2002. Molecular cytogenetic characterization of a 10p14 deletion that includes the DGS2 region in a patient with multiple anomalies. Am J Med Genet 113: 207–212.

Swillen A, Vogels A, Devriendt K, Fryns JP. 2000. Chromosome 22q11 deletion syndrome: Update and review of the clinical features, cognitive-behavioral spectrum, and psychiatric complications. Am J Med Genet 97:128–135.

Thakker RV. 2008. GATA3 and hypoparathyroidism, deafness and renal disease. In: Epstein CJ, Erickson RP, Wynshaw-Boris A, editors. Inborn errors of development, 2nd edition. New York: Oxford University Press. pp 1055-1060.

Ting C-N, Olson MC, Barton KP, Leiden JM. 1996. Transcription factor GATA-3 is required for development of the T-cell lineage. Nature 384:474–478.

Van Esch H, Groenen P, Nesbit MA, Schuffenhauer S, Lichtner P, Vanderlinden G, Harding B, Beetz R, Bilous RW, Holdaway I, Shaw NJ, Fryns JP, Van de Ven W, Thakker RV, Devriendt K. 2000. GATA3 haploinsufficiency causes human HDR syndrome. Nature 406:419–422.

Yagi H, Furutani Y, Hamada H, Sasaki T, Asakawa S, Minoshima S, Ichida F, Joo K, Kimura M, Imamura S, Kamatani N, Momma K, Takao A, Nakazawa M, Shimizu N, Matsuoka R. 2003. Role of TBX1 in human del22q11.2 syndrome. Lancet 362:1366–1373.

Yatsenko SA, Yatsenko AN, Szigeti K, Craigen WJ, Stankiewicz P, Cheung SW, Lupski JR. 2004. Interstitial deletion of 10p and atrial septal defect in DiGeorge 2 syndrome. Clin Genet 66:128–136.

Zahirieh A, Nesbit MA, Ali A, Wang K, He N, Stangou M, Bamichas G, Sombolos K, Thakker RV, Pei Y. 2005. Functional analysis of a novel GATA3 mutation in a family with the hypoparathyroidism, deafness, and renal dysplasia syndrome. J Clin Endocrinol Metab 90:2445–2450.

RESEARCH ARTICLE

AMERICAN JOURNAL OF medical genetics A

MLL2 and *KDM6A* Mutations in Patients With Kabuki Syndrome

Noriko Miyake,[1]* Eriko Koshimizu,[1] Nobuhiko Okamoto,[2] Seiji Mizuno,[3] Tsutomu Ogata,[4] Toshiro Nagai,[5] Tomoki Kosho,[6] Hirofumi Ohashi,[7] Mitsuhiro Kato,[8] Goro Sasaki,[9] Hiroyo Mabe,[10] Yoriko Watanabe,[11] Makoto Yoshino,[11] Toyojiro Matsuishi,[11] Jun-ichi Takanashi,[12] Vorasuk Shotelersuk,[13] Mustafa Tekin,[14] Nobuhiko Ochi,[15] Masaya Kubota,[16] Naoko Ito,[17] Kenji Ihara,[17] Toshiro Hara,[17] Hidefumi Tonoki,[18] Tohru Ohta,[19] Kayoko Saito,[20] Mari Matsuo,[20] Mari Urano,[20] Takashi Enokizono,[21] Astushi Sato,[22] Hiroyuki Tanaka,[23] Atsushi Ogawa,[24] Takako Fujita,[25] Yoko Hiraki,[26] Sachiko Kitanaka,[22] Yoichi Matsubara,[27] Toshio Makita,[28] Masataka Taguri,[29] Mitsuko Nakashima,[1] Yoshinori Tsurusaki,[1] Hirotomo Saitsu,[1] Ko-ichiro Yoshiura,[30] Naomichi Matsumoto,[1]* and Norio Niikawa[19]

[1]Department of Human Genetics, Yokohama City University Graduate School of Medicine, Yokohama, Japan

[2]Department of Medical Genetics, Osaka Medical Center and Research Institute for Maternal and Child Health, Izumi, Japan

[3]Department of Pediatrics, Central Hospital, Aichi Human Service Center, Kasugai, Japan

[4]Department of Pediatrics, Hamamatsu University School of Medicine, Hamamatsu, Japan

[5]Department of Pediatrics, Dokkyo Medical University Koshigaya Hospital, Saitama, Japan

[6]Department of Medical Genetics, Shinshu University School of Medicine, Matsumoto, Japan

[7]Division of Medical Genetics, Saitama Children's Medical Center, Iwatsuki, Japan

[8]Department of Pediatrics, Yamagata University Faculty of Medicine, Yamagata, Japan

[9]Department of Pediatrics, Tokyo Dental College Ichikawa General Hospital, Chiba, Japan

[10]Department of Child Development, Kumamoto University Hospital, Kumamoto, Japan

[11]Department of Pediatrics and Child Health, Kurume University School of Medicine, Kurume, Japan

[12]Department of Pediatrics, Kameda Medical Center, Kamogawa, Chiba, Japan

[13]Center of Excellence for Medical Genetics, Department of Pediatrics, Faculty of Medicine, Chulalongkorn University, Bangkok, Thailand

[14]John P. Hussman Institute for Human Genomics, Miller School of Medicine, University of Miami, Miami, Florida

[15]Department of Pediatrics, Aichi Prefectural Hospital and Habilitation Center for Disabled Children, Dai-ni Aoitori Gakuen, Okazaki, Japan

[16]Division of Neurology, National Center for Child Health and Development, Tokyo, Japan

[17]Department of Pediatrics, Graduate School of Medical Sciences, Kyushu University, Fukuoka, Japan

[18]Section of Clinical Genetics, Department of Pediatrics, Tenshi Hospital, Sapporo, Japan

[19]Research Institute of Personalized Health Sciences, Health Science University of Hokkaido, Tobetsu, Japan

[20]Institute of Medical Genetics, Tokyo Women's Medical University, Tokyo, Japan

[21]Department of Pediatrics, University of Tsukuba Hospital, Tsukuba, Japan

[22]Department of Pediatrics, Graduate School of Medicine, The University of Tokyo, Tokyo, Japan

[23]Department of Pediatrics, Ohta Nishinouchi Hospital, Tokyo, Japan

[24]Department of Pediatrics, Chikushi Hospital, Fukuoka University, Fukuoka, Japan

[25]Department of Pediatrics, Fukuoka University School of Medicine, Fukuoka, Japan

[26]Hiroshima Municipal Center for Child Health and Development, Hiroshima, Japan

[27]Department of Medical Genetics, Tohoku University School of Medicine, Sendai, Japan

[28]Education Center, Asahikawa Medical University, Asahikawa, Japan

[29]Department of Biostatistics and Epidemiology, Yokohama City University Graduate School of Medicine, Yokohama, Japan

[30]Department of Human Genetics, Graduate School of Biomedical Sciences, Nagasaki University, Nagasaki, Japan

Manuscript Received: 9 January 2013; Manuscript Accepted: 9 May 2013

Kabuki syndrome is a congenital anomaly syndrome characterized by developmental delay, intellectual disability, specific facial features including long palpebral fissures and ectropion of the lateral third of the lower eyelids, prominent digit pads, and skeletal and visceral abnormalities. Mutations in *MLL2* and *KDM6A* cause Kabuki syndrome. We screened 81 individuals with Kabuki syndrome for mutations in these genes by conventional methods (n = 58) and/or targeted resequencing (n = 45) or whole exome sequencing (n = 5). We identified a mutation in *MLL2* or *KDM6A* in 50 (61.7%) and 5 (6.2%) cases, respectively. Thirty-five *MLL2* mutations and two *KDM6A* mutations were novel. Non-protein truncating-type *MLL2* mutations were mainly located around functional domains, while truncating-type mutations were scattered through the entire coding region. The facial features of patients in the *MLL2* truncating-type mutation group were typical based on those of the 10 originally reported patients with Kabuki syndrome; those of the other groups were less typical. High arched eyebrows, short fifth finger, and hypotonia in infancy were more frequent in the *MLL2* mutation group than in the *KDM6A* mutation group. Short stature and postnatal growth retardation were observed in all individuals with *KDM6A* mutations, but in only half of the group with *MLL2* mutations. © 2013 Wiley Periodicals, Inc.

Key words: Kabuki syndrome; *MLL2*; *KDM6A*; mutation; genotype–phenotype correlation

How to Cite this Article:
Miyake N, Koshimizu E, Okamoto N, Mizuno S, Ogata T, Nagai T, Kosho T, Ohashi H, Kato M, Sasaki G, Mabe H, Watanabe Y, Yoshino M, Matsuishi T, Takanashi J-i, Shotelersuk V, Tekin M, Ochi N, Kubota M, Ito N, Ihara K, Hara T, Tonoki H, Ohta T, Saito K, Matsuo M, Urano M, Enokizono T, Sato A, Tanaka H, Ogawa A, Fujita T, Hiraki Y, Kitanaka S, Matsubara Y, Makita T, Taguri M, Nakashima M, Tsurusaki Y, Saitsu H, Yoshiura K-i, Matsumoto N, Niikawa N. 2013. *MLL2* and *KDM6A* mutations in patients with Kabuki syndrome.
Am J Med Genet Part A 161A:2234–2243.

INTRODUCTION

Kabuki syndrome (KS; OMIM 147920) is a multiple congenital anomaly syndrome that was originally reported by Niikawa et al. [1981] and Kuroki et al. [1981] (also known as Kabuki make-up syndrome or Niikawa–Kuroki syndrome). KS is diagnosed clinically by characteristic facial features, including long palpebral fissures and ectropion of the lateral third of the lower eyelids, postnatal growth impairment (short stature), developmental delay, intellectual disability, dermatoglyphic abnormalities, visceral and skeletal abnormalities, and immunological dysfunction. The prevalence of the disorder is estimated to be 1 in 32,000 live births [Niikawa et al., 1988]. Two genes have shown to be mutated in patients with KS: *MLL2* (myeloid/lymphoid or mixed-lineage leukemia 2; NM_003482.3) at 12q13.12 and *KDM6A* (lysine (K)-specific demethylase 6A; NM_021140.2) at Xp11.3 [Ng et al., 2010; Lederer et al., 2012; Miyake et al., 2013]. *MLL2* encodes a histone H3 lysine 4 (H3K4)-specific methyl transferase and KDM6A is a specific demethylase of histone H3 lysine 27 (H3K27) [Prasad et al., 1997; Lee et al., 2007]. They are both trithorax group proteins and bind each other [Schuettengruber et al., 2007]. These proteins are important for the chromatin state and transcription activation: MLL2 methylates H3K4 and KMD6A removes the H3K27 trimethylation repressive mark [Dubuc et al., 2013]. The loss of MLL2 or KDM6A function may lead to repressed transcription [Dubuc et al., 2013].

To our knowledge, there has been no comprehensive screen for mutations in these two genes in the same patient series. In this report, we performed a mutation screen of both genes in 81 patients with KS. We then evaluated the clinical features based on the genetic information.

MATERIALS AND METHODS

Samples

Eighty-one individuals clinically suspected to have KS were incorporated in this study: 77 Japanese, two Caucasians, one Belgian, and one Thai. They were all sporadic except for KMS-79, who had an affected sibling. Peripheral blood samples or saliva samples from the

Additional supporting information may be found in the online version of this article at the publisher's web-site.

Conflict of interest: none.
Grant sponsor: Ministry of Health, Labour and Welfare of Japan; Grant sponsor: Japan Science and Technology Agency; Grant sponsor: Strategic Research Program for Brain Sciences; Grant sponsor: Ministry of Education, Culture, Sports, Science and Technology of Japan; Grant sponsor: Grant-in-Aid for Scientific Research from the Japan Society for the Promotion of Science; Grant sponsor: Grant-in-Aid for Young Scientists from the Japan Society for the Promotion of Science; Grant sponsor: Takeda Science Foundation; Grant sponsor: Yokohama Foundation for the Advancement of Medical Science; Grant sponsor: Hayashi Memorial Foundation for Female Natural Scientists.

*Correspondence to:
Dr. Noriko Miyake or Prof. Naomichi Matsumoto, Department of Human Genetics, Yokohama City University Graduate School of Medicine, 3-9 Fukuura, Kanazawa-ku, Yokohama 236-0004, Japan.
E-mails: nmiyake@yokohama-cu.ac.jp (N. Miyake) or naomat@yokohama-cu.ac.jp (N. Matsumoto)

Article first published online in Wiley Online Library (wileyonlinelibrary.com): 2 August 2013
DOI 10.1002/ajmg.a.36072

patients and their parents (when available) were collected with informed consent and DNA was extracted using a QuickGene-610L (Fujifilm, Tokyo, Japan) or Oragene-DNA kit (DNA Genotek, Inc., Ottawa, Canada) according to the manufacturer's instructions. This study included four previously reported patients (KMS-50, KMS-51, KMS-61, and KMS-71) [Tekin et al., 2006; Torii et al., 2009; Ito et al., 2012]. In addition, three patients with a *KDM6A* mutation were previously described as Patients 1, 2, and 3 by Miyake et al. [2013], and are named KMS-31, KMS-37, and KMS-65, respectively, in this report. This study was approved by the Institutional Review Board of Yokohama City University School of Medicine.

Mutation Screening

Fifty-eight patients (KMS-01 to KMS-69) were screened for *MLL2* mutations by the high-resolution melting (HRM) method using a LightCycler 480 System II (Roche Diagnostics, Indianapolis, IN) and subsequent Sanger sequencing. If an HRM curve pattern was different from those of controls, the DNA sample was Sanger sequenced on an ABI 3500xl or 3130xl Genetic Analyzer (Applied Biosystems, Foster City, CA) and the sequences were analyzed using Sequencher software version 4.10.1 (Gene Codes Corporation, Ann Arbor, MI). *KDM6A* was analyzed in samples with no *MLL2* mutation using HRM analysis and Sanger sequencing as above (n = 37). For male samples, genotyping using spike-in control male genomic DNA (10%) was performed to detect a hemizygous mutation. The latter 23 patients (KMS-70 to KMS-92), as well as 22 patients with no mutation in either gene detected by conventional methods, were analyzed by targeted resequencing as described in the following section. We judged a variant as pathogenic when it was previously reported to cause KS, or novel variant when it was not observed in unaffected parents or in in-house exome data (n = 977), dbSNP135, or EVS6500 (Exome Variant Server, NHLBI GO Exome Sequencing Project, Seattle, WA; http://evs.gs.washington.edu/EVS/; accessed March 1, 2013). In addition, the missense mutation predicted to be polymorphism by both of two predictions (Polyphen-2: http://genetics.bwh.harvard.edu/pph2/ [Adzhubei et al., 2010] and MutationTaster: http://www.mutationtaster.org/ [Schwarz et al., 2010]) was considered to be non-pathogenic. Parentage analysis was conducted for the patients only when the parental samples were available. TaKaRa Ex Taq and TaKaRa LA Taq (both Takara, Tokyo, Japan) were used for amplification. The primer sequences and PCR conditions are available on request. All pathological variants were confirmed by Sanger sequencing. Nucleotide numbering reflects cDNA numbering with +1 corresponding to the A of the ATG translation initiation codon in the reference sequence (RefSeq NM_003482.3 for *MLL2*, RefSeq NM_021140.2 for *KDM6A*).

Targeted Resequencing of *MLL2* and *KDM6A* by Next-Generation Sequencing

Ion AmpliSeq Custom Panels (Life Technologies, Inc., Grand Island, NY) covering the entire coding region of *MLL2* and *KDM6A* were created via the Ion AmpliSeq Designer v1.2 (https://ampliseq.com/browse.action). Libraries were prepared using the Ion AmpliSeq Library Kit 2.0 (Life Technologies, Inc.), with 10 ng of genomic DNA for each primer pool (two pools for this analysis). An Agilent 2200 TapeStation (Agilent Technologies, Santa Clara, CA) and the associated High Sensitivity D1K Screen Tape (Agilent Technologies) were used to check the size distribution and the concentration of the DNA libraries. Emulsion PCR and enrichment steps were carried out using the Ion OneTouch 200 Template Kit v2 (Life Technologies, Inc.). The amplicon libraries were sequenced on an Ion Torrent Personal Genome Machine system using 314 or 316 chips, and bar-coding was applied with an Ion Xpress Barcode Adapters 1–16 Kit (all Life Technologies, Inc.). Torrent Suite 2.2 (Life Technologies, Inc.) was used for mapping, base calling, and variant calling. Sequences were annotated using SeattleSeq Annotation 134 (http://snp.gs.washington.edu/SeattleSeqAnnotation134/). All variants were confirmed by Sanger sequencing.

Whole Exome Sequencing by High-Throughput Next-Generation Sequencing

Whole exome sequencing was performed in five individuals (KMS-09, -18, -21, -23, and -61) who had no *MLL2* or *KDM6A* abnormality by HRM analysis. DNA was processed with a SureSelect Human All Exon V4 kit (Agilent Technologies), sequenced on a HiSeq2000 (Illumina, Inc., San Diego, CA), and analyzed as previously described [Tsurusaki et al., 2013]. Variants in *MLL2* and *KDM6A* were confirmed by Sanger sequencing.

X-Inactivation Assay

X-inactivation analysis was performed as described [Allen et al., 1992] with slight modification. Briefly, genomic DNA (500 ng) was digested with two methylation-sensitive restriction enzymes, *Hpa*II and *Hha*I (New England Biolabs, Beverly, MA), and purified by phenol/chloroform extraction and ethanol precipitation. Digested and undigested DNA samples (10 ng) were separately amplified for the (CAG)*n* polymorphism at the androgen receptor locus. The forward primer was labeled with 5′ FAM dye. PCR products were analyzed on an ABI 3500xl Genetic Analyzer using GeneMapper Software Version 4.1 (Applied Biosystems). The assay was independently performed twice.

cDNA Sequencing

Total RNA was extracted from a lymphoblastoid cell line established from KMS-81 (c.1909_1912del in *KDM6A*) using an RNeasy Plus mini kit (Qiagen, Hilden, Germany) with and without cycloheximide treatment (30 μg/ml) for 4 hr before cell collection. Reverse transcription (RT) was performed using a Superscript III First-Strand synthesis system for RT-PCR (Life Technologies, Inc.). As the mutation was located in exon 17, the region from the exon 15/16 boundary to the exon 17/18 boundary of *KDM6A* was amplified using cDNA-specific primer pairs (sequences available on request) and sequenced by the Sanger method.

Statistical Analysis

The frequencies of clinical features in the two groups were compared by Fisher's exact test. A difference was considered statistically

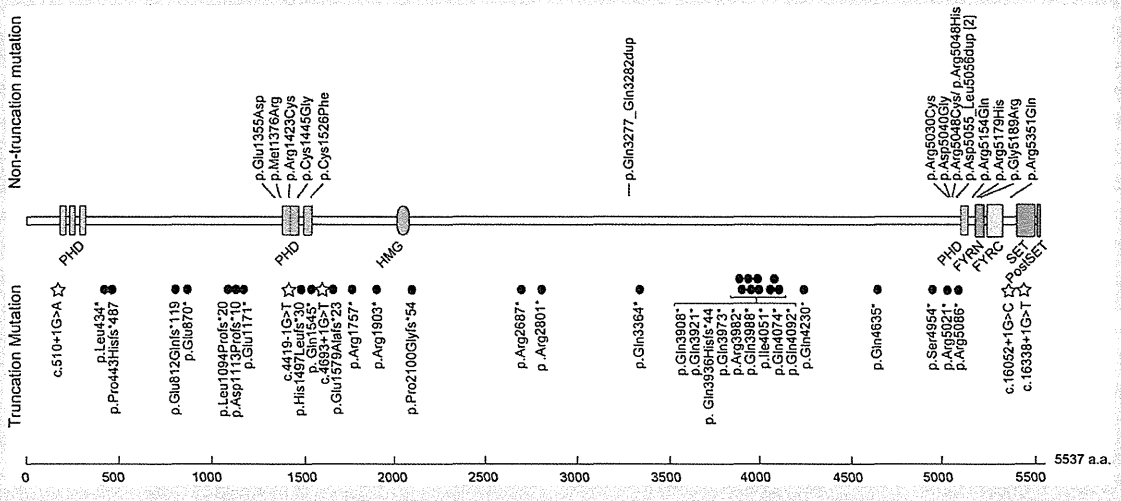

FIG. 1. ***MLL2*** **mutations in patients with Kabuki syndrome. Upper: Non-truncating-type mutations. Middle: MLL2 protein structure with functional domains. The protein contains seven plant homeodomains (PHD), one high-mobility group (HMG) domain, a Phe-Tyr-rich *N*-terminal (FYRN) domain, a Phe-Tyr-rich *C*-terminal (FYRC) domain, a SET (Suvar3-9, Enhancer-of-zeste, Trithorax) domain, and a PostSET domain. These functional domains were based on a prediction by SMART (http://smart.embl-heidelberg.de/) and the UniProtKB database (http://www.uniprot.org/uniprot/O14686). Lower: Truncating-type mutations. Black circles denote nonsense mutations or frameshift mutations. Stars represent splice-site mutations.**

significant if $P < 0.05$. Correction for multiple testing was not applied.

RESULTS

Overall Mutation Detection Rates

Pathogenic mutations in *MLL2* and *KDM6A* were found in 50 (61.7%) and five (6.2%) of the 81 patients with KS, respectively (Figs. 1 and 2, Tables I and II). Of the 50 *MLL2* mutations, 35 (70.0%) were predicted to be protein truncating-type and 15 (30.0%) were predicted to be non-truncating-type. Interestingly, non-truncating mutations were mostly localized in or adjacent to the functional domains, while truncating mutations were scattered throughout the entire coding region (Fig. 1). Fifteen of the *MLL2* mutations have been previously reported (Table I). Three novel variants (not included in the 50 mutations) were considered non-pathogenic (Supplemental Table I). Variant c.10942C > G in patient KMS-22 was predicted to be benign by Polyphen-2 and MutationTaster, c.8813C > T in patient KMS-62 was inherited from an unaffected father, and c.4065A > T in KMS-75 was found heterozygously in our 977 in-house controls. An in-frame duplication in patients KMS-40 and KMS-62, which predicted p.Asp5055_Leu5056dup, was predicted to be polymorphic by MutationTaster, but was previously reported as a pathogenic mutation [Micale et al., 2011]. In addition, the other in-frame mutation in KMS-02 was also predicted to be polymorphic. Unfortunately, parental samples were unavailable for these individuals, except for the mother of patient KMS-62, who did not have this mutation; thus, the de novo status remains unclear. Of the five *KDM6A* mutations including three mutations reported previously [Miyake et al., 2013], four were truncating-type and one was an in-frame deletion located within the Jumonji C domain (Fig. 2).

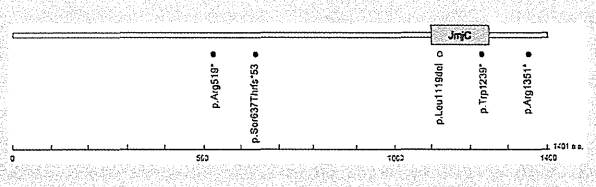

FIG. 2. ***KDM6A*** **mutations in patients with Kabuki syndrome. Upper: Scheme of KDM6A protein. It contains a Jumonji C (JmjC) domain (purple box). Lower: Black circles indicate truncating-type mutations (nonsense or frameshift mutations); the white circle represents a non-truncating-type mutation (in-frame deletion).**

Clinical Comparison Between the Mutation-Positive and -Negative Groups

We compared the clinical features of the *MLL2* or *KDM6A* mutation-positive and -negative groups (Supplemental Table II). Long palpebral fissures were observed in almost all patients. Cleft lip/palate was more frequently observed in the mutation-positive group ($P = 0.0197$). Interestingly, developmental delay and intellectual disability were observed in all individuals with mutations but were unobserved in some mutation-negative cases ($P = 0.0314$